EFFICIENT DIFFUSION TRANSFORMER POLICIES WITH MIXTURE OF EXPERT DENOISERS FOR MULTITASK LEARNING

Anonymous authors
Paper under double-blind review

ABSTRACT

Diffusion Policies have become widely used in Imitation Learning, offering several appealing properties, such as generating multimodal and discontinuous behavior. As models are becoming larger to capture more complex capabilities, their computational demands increase, as shown by recent scaling laws. Therefore, continuing with the current architectures will present a computational roadblock. To address this gap, we propose Mixture-of-Denoising Experts (MoDE) as a novel policy for Imitation Learning. MoDE surpasses current state-of-the-art Transformer-based Diffusion Policies while enabling parameter-efficient scaling through sparse experts and noise-conditioned routing, reducing both active parameters by 40% and inference costs by 80% via expert caching. Our architecture combines this efficient scaling with noise-conditioned self-attention mechanism, enabling more effective denoising across different noise levels. MoDE achieves state-of-the-art performance across 134 tasks in four established imitation learning benchmarks (CALVIN and LIBERO). Notably, by pretraining MoDE on diverse robotics data, we achieve a new state-of-the-art result of 3.98 on CALVIN and 0.95 on LIBERO-90. It surpasses both CNN-based and Transformer Diffusion Policies by an average of 20% in all settings, while using 80% fewer FLOPs and fewer active parameters. Furthermore, we conduct comprehensive ablations on MoDE's components, providing insights for designing efficient and scalable Transformer architectures for Diffusion Policies.

1 INTRODUCTION

Diffusion models learn to reverse an iterative process that adds Gaussian noise to data samples (Ho et al., 2020; Song et al., 2020). After training, they can generate new samples conditioned on goals like instructions or images. Recently, diffusion models have gained widespread adoption as policies for Imitation Learning (IL) (Octo Model Team et al., 2023; Reuss et al., 2023; Chi et al., 2023). IL is a powerful paradigm to train agents from expert demonstrations to learn versatile skills (Pomerleau, 1989; Nair et al., 2017; Pari et al., 2021; Fu et al., 2024).

Diffusion policies offer several appealing properties for IL: they can generate diverse multimodal behavior (Jia et al., 2024), scale with more data (Octo Model Team et al., 2023), and handle discontinuities in the action space (Chi et al., 2023). However, a major limitation is their high computational cost, resulting in slower training and inference speed as models become larger. Standard architectures contain hundreds of millions of parameters (Chi et al., 2023) and require many denoising steps to generate actions. Large encoder modules for images and text further increase the computational requirements for IL policies. This restricts their use in real-time robotics applications, particularly in scenarios with limited on-board computing resources, such as mobile robots.

To address these challenges, we explore Mixture-of-Experts (MoE) that can scale model capacity while using fewer FLOPs for training and inference. The core idea behind a sparse MoE is to utilize only a subset of the total model parameters during each forward pass. This is achieved by having multiple expert subnetworks and a routing model, that sparsely activates experts and interpolates their outputs, based on the input.

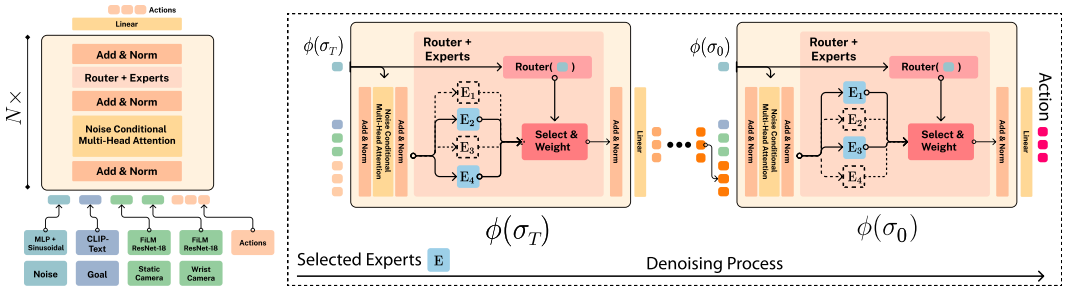

Figure 1: The proposed MoDE architecture (left) uses a transformer with causal masking, where each block includes noise-conditional self-attention and a noise-conditioned router that assigns tokens to expert models based on the noise level. This design enables efficient, scalable action generation. On the right, the router's activation of subsets of simple MLP experts with Swish-GLU activation during denoising is illustrated.

We introduce **M**ixture-of-**D**enoising **E**xperts Policy (MoDE), a scalable and efficient MoE Diffusion Policy.

Our work is inspired by prior results showcasing the multitask nature of the denoising process (Hang et al., 2024), where there is little transfer between the different phases in the denoising process. We present a novel noise-conditioned routing mechanism, that distributes tokens to our experts based on the current noise level. MoDE leverages noise-conditioned self-attention combined with a noise input token for enhanced noise-injection. Our proposed Policy surpasses previous Diffusion Policies with higher efficiency and demonstrates sota performance across 134 diverse tasks in challenging goal-conditioned imitation learning benchmarks: CALVIN (Mees et al., 2022b) and LIBERO (Liu et al., 2023). Through comprehensive ablation studies, we investigate the impact of various design decisions, including token routing strategies, noise-injection techniques, expert distribution and diverse pretraining on a large-scale robot dataset Collaboration et al. (2023). We summarize our contributions below:

- We introduce MoDE, a novel Mixture-of-Experts Diffusion Policy that achieves state-of-the-art performance while using 80% fewer FLOPs and less active parameters than dense transformer baselines thanks to our noise-based expert caching and sparse MoE design.
- We demonstrate MoDE's effectiveness across 134 tasks in 4 benchmarks, showing an average 20% performance increase over prior Diffusion Policies while maintaining improved computational efficiency.
- We present detailed ablation studies that investigate the importance of routing strategies and noise-injection, visualizing expert utilization across denoising steps to identify key components of MoDE.

2 Related Work

Diffusion in Robotics. In recent years, Diffusion Models (Song & Ermon, 2019; Ho et al., 2020; Karras et al., 2022) have gained widespread adoption in the context of robotics. They are used as a policy representation for Imitation Learning (Chi et al., 2023; Reuss et al., 2023; Xian et al., 2023; Ke et al., 2024; Li et al., 2023b; Scheikl et al., 2023) and in Offline Reinforcement Learning (Ajay et al., 2023a; Janner et al., 2022; Pari et al., 2022). Other applications of diffusion models in robotics include robot design generation (Wang et al., 2023), video-generation (Du et al., 2023; Ko et al., 2023; Ajay et al., 2023b) and motion planning (Carvalho et al., 2023; Urain et al., 2023). The most common architecture for using diffusion models as a policy in robotics is a Convolutional neural network (CNN) with additional FiLM conditioning (Perez et al., 2018) to guide the generation based on context information. Recently, the transformer architecture has been adopted as a strong alternative backbone for diffusion policies, specifically in IL. Examples include Octo (Octo Model Team et al., 2023), BESO (Reuss et al., 2023) and 3D-Diffusion-Actor (Ke et al., 2024). However, no prior work considers using a Mixture of Experts architecture for improving the computational efficiency and inference time and solely relies on dense transformer architectures.

Mixture-of-Experts. MoE are a class of models where information is selectively routed through the model. The modern version of MoE was introduced in (Shazeer et al., 2017), where a routing or gating network conditionally chooses a subset of experts to send an input to. After Transformers (Vaswani et al., 2017) proved to be an effective model that scales well with data, they were modified to have expert feed-forward networks at each block of the model in (Fedus et al., 2022) which presented Switch Transformers. Switch Transformers laid the groundwork that is still widely adopted in different Large-Language-Models (LLM) (Jiang et al., 2024; Du et al., 2022). This allowed for more total parameters while keeping the forward and backward FLOPs smaller than their dense counterpart, thus yielding significant performance gains. However, training both the router and experts in parallel is a non-trivial optimization problem, and it can yield suboptimal solutions such as expert collapse where experts learn similar functions instead of specializing (Chi et al., 2022). In addition, router collapse occurs when the router selects a small subset of the experts and doesn't utilize all the experts. This is mitigated with load balancing losses (Shazeer et al., 2017; Fedus et al., 2022) which encourage the router to distribute inputs more evenly across experts. Multiple works have explored different methods to perform routing, such as expert choice routing (Zhou et al., 2022), differential k-selection (Hazimeh et al., 2021), frozen hashing functions (Roller et al., 2021), and linear assignment (Lewis et al., 2021).

Multi Task Learning in Diffusion Models. It has been shown that the denoising process is multi-task Hang et al. (2024). Leveraging this idea, works have taken architectures that are suited for multi-task learning. Some works have explicitly scheduled which parameters are specialized to which stage in the denoising process (Park et al., 2023; Go et al., 2023). In extension to this (Park et al., 2024) uses the scheduling as guidance during training but also learns how to modulate representations based on the denoising stage. Finally, some works have employed different architectures based on the denoising stage (Lee et al., 2024b).

3 METHOD

In this section, we introduce MoDE, our novel MoE Diffusion Policy. First, we formulate the problem of learning a policy for IL. Next, we summarize the framework used in Diffusion Policies and then introduce our MoDE architecture with our novel noise-conditioned routing and noise-conditioned self-attention that enable efficient policy design. Finally, we explain our expert caching mechanism for efficient inference and explain the pretraining of MoDE.

3.1 PROBLEM FORMULATION

We consider the problem of learning a language-conditioned policy $\pi_\theta(\bar{\boldsymbol{a}}|\bar{\boldsymbol{s}}, \boldsymbol{g})$ given a dataset of robot demonstrations $\mathcal{T}$. The policy predicts a sequence of future actions $\bar{\boldsymbol{a}} = (\boldsymbol{a}, \ldots, \boldsymbol{a}_{i+j-1})$ of length j, conditioned on the history of state embeddings $\bar{\boldsymbol{s}} = (\boldsymbol{s}_{i-h+1}, \ldots, \boldsymbol{s}_i)$ of length h and a desired goal $\boldsymbol{g}$. The dataset contains $\tau \in \mathcal{T}$ trajectories, where trajectory consists of a sequence of triplets of state, actions, and goal $(\bar{\boldsymbol{s}}_i, \boldsymbol{a}_i, \boldsymbol{g})$. $\boldsymbol{g}$ is a language instruction. Our policy is trained to maximize the log-likelihood of the action sequence given the context of state history and goal:

$$\mathcal{L}_{\text{IL}} = \mathbb{E}\left[\sum_{(\bar{\boldsymbol{s}}, \bar{\boldsymbol{a}}, \boldsymbol{g}) \in \mathcal{T}} \log \pi_\theta\left(\bar{\boldsymbol{a}}|\bar{\boldsymbol{s}}, \boldsymbol{g}\right)\right]. \tag{1}$$

3.2 DIFFUSION POLICY

MoDE uses the continuous-time diffusion model of EDM (Karras et al., 2022) as a policy representation. Diffusion models are a type of generative model for generating data by initially adding noise through Gaussian perturbations and then reversing this process. MoDE applies the score-based diffusion model to represent the policy $\pi_\theta(\bar{\boldsymbol{a}}|\bar{\boldsymbol{s}}, \boldsymbol{g})$. The perturbation and inverse process can be described using a stochastic differential equation:

$$\mathrm{d}\bar{\boldsymbol{a}} = \left(\beta_t \sigma_t - \dot{\sigma}_t\right) \sigma_t \nabla_a \log p_t(\bar{\boldsymbol{a}}|\bar{\boldsymbol{s}}, \boldsymbol{g}) dt + \sqrt{2\beta_t} \sigma_t d\omega_t, \tag{2}$$

where β_t controls the noise injection, $d\omega_t$ refers to infinitesimal Gaussian noise, and $p_t(\bar{\boldsymbol{a}}|\bar{\boldsymbol{s}}, \boldsymbol{g})$ is the score function of the diffusion process, that moves samples away from regions of high-data density in

the forward process. To generate new samples from noise a neural network is trained to approximate the score function $\nabla_{\bar{\boldsymbol{a}}} \log p_t(\bar{\boldsymbol{a}}|\bar{\boldsymbol{s}}, \boldsymbol{g})$ via Score matching (SM) (Vincent, 2011)

$$\mathcal{L}_{\text{SM}} = \mathbb{E}_{\sigma,\bar{\boldsymbol{a}},\boldsymbol{\epsilon}}\big[\alpha(\sigma_t)\|D_\theta(\bar{\boldsymbol{a}} + \boldsymbol{\epsilon}, \bar{\boldsymbol{s}}, \boldsymbol{g}, \sigma_t) - \bar{\boldsymbol{a}}\|_2^2\big], \tag{3}$$

where $D_\theta(\bar{\boldsymbol{a}} + \boldsymbol{\epsilon}, \bar{\boldsymbol{s}}, \boldsymbol{g}, \sigma_t)$ is the trainable neural network. During training, we sample noise from a training distribution and add it to an action sequence. The network predicts the denoised actions and computes the SM loss.

After training, we can generate a new action sequence starting from random noise by approximating the reverse SDE or related ODE in discrete steps using numerical ODE integrators. Therefore, we sample noise from the prior $\boldsymbol{a}_T \sim \mathcal{N}(\mathbf{0}, \sigma_T^2\mathbf{I})$ and iteratively denoise it. MoDE uses the DDIM-solver, a numerical ODE-solver designed for diffusion models (Song et al., 2021), that allows fast denoising of actions in a few steps. MoDE uses 10 denoising steps in all our experiments.

3.3 Mixture-of-Experts Denoising

We now introduce MoDE, a novel approach that employs noise-conditioned expert routing to enhance diffusion-based policies. This novel routing mechanism enables us to precompute and fuse required experts for more efficient inference. An overview of MoDE's architecture with the routing mechanism is shown in Figure 1.

For language conditioning, MoDE leverages a frozen CLIP language encoder to generate a latent goal vector, while image encoding utilizes FiLM-conditioned ResNets-18/50. The model processes a sequence of input tokens $\mathbf{X} \in \mathbb{R}^{\text{tokens}\times\mathbf{D}}$ and noise level σ_t. A linear projection layer $\phi(\sigma_t)$ encodes the noise level into a token, which is incorporated into $\mathbf{X}$. The complete MoDE architecture, $\text{MoDE}(\mathbf{X}, \phi(\sigma_\mathbf{t}))$, consists of L transformer blocks, each specialized for different denoising phases.

We now define each block f^i as a composition of a self-attention (SA) layer and an MoE layer,

$$f^i(\mathbf{X}, \phi(\sigma_\mathbf{t})) = \text{MoE}(\text{SA}(\hat{\mathbf{X}}) + \mathbf{X}, \phi(\sigma_\mathbf{t})) + \mathbf{X}. \tag{4}$$

A key change in our approach is the integration of noise-aware positional embeddings. By adding $\phi(\sigma_t)$ to all tokens in $\mathbf{X}$ before self-attention:

$$\hat{\mathbf{X}} = \phi(\sigma_t) + \mathbf{X}, \tag{5}$$

we enable each token to adapt its attention patterns based on the current denoising phase. This design enhances denoising performance without introducing additional parameters or architectural complexity.

The self-attention mechanism follows the standard formulation (Vaswani et al., 2017):

$$\text{SA}(\hat{\mathbf{X}}) = \text{softmax}(\frac{1}{\sqrt{D}}[\hat{\mathbf{X}}W_Q][\hat{\mathbf{X}}W_K]^T)[\hat{\mathbf{X}}W_V]. \tag{6}$$

Our MoE layer introduces a novel noise-conditioned routing strategy. Given N experts $\mathbf{E_i} i = 1^N$, the layer output is:

$$\text{MoE}(\mathbf{X}, \phi(\sigma_\mathbf{t})) = \sum \mathbf{i} = \mathbf{1^N}\mathbf{R}(\phi(\sigma_\mathbf{t}))\mathbf{E_i}(\mathbf{X}), \tag{7}$$

where the routing function $\mathbf{R}(\cdot) : \mathbb{R}^{\text{tokens}\times\mathbf{D}} \to \mathbb{R}^{\text{tokens}\times\mathbf{N}}$ determines expert selection:

$$\mathbf{R}(\phi(\sigma_\mathbf{t})) = \text{topk}(\text{softmax}(\phi(\sigma_\mathbf{t})\mathbf{W_R}), k) \tag{8}$$

Unlike traditional MoE approaches that route based on input content, MoDE's routing mechanism specifically considers the noise level. This enables specialized experts for different denoising phases, allowing for both improved performance and computational efficiency through expert caching (detailed in subsubsection 3.3.1). We implement topk using multinomial sampling without replacement, selecting *k* elements according to $\text{softmax}(\phi(\sigma_t)W_R)$ probabilities. To maintain gradient flow through the non-differentiable sampling process, we scale expert outputs by routing probabilities and renormalize the selected probabilities. To prevent expert collapse, we incorporate a load balancing loss (LB) (Fedus et al., 2022):

$$LB(\sigma_t) = N\sum_{n=1}^{N}\frac{1}{|\mathcal{B}|}(\sum_{i=1}^{|\mathcal{B}|}\mathbb{1}\mathbf{R}(\phi(\sigma_{\mathbf{t_i}}))\mathbf{n} > \mathbf{0})\frac{1}{|\mathcal{B}|}(\sum i = 1^{|\mathcal{B}|}\text{softmax}(\phi(\sigma_{t_i})W_R)_n) \tag{9}$$

with $\gamma = 0.01$ as the balancing coefficient.

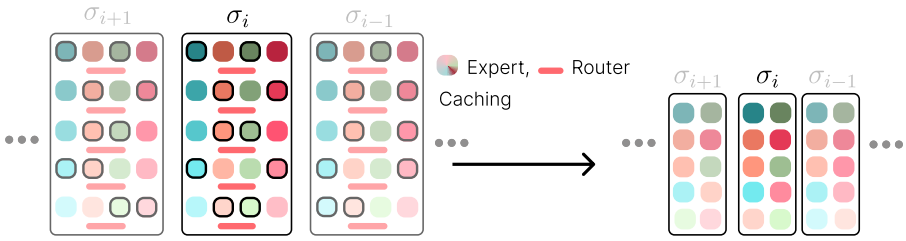

Figure 2: After training MoDE, the router is noise-conditioned, allowing pre-computation of the experts used at each noise level before inference. This enables removing the router and retaining only the selected experts, significantly improving network efficiency.

3.3.1 Router and Expert Caching

To make our method more efficient, we exploit the fact that our MoE is noise-conditioned, meaning that at each noise level, the routing path is deterministic and can be precomputed. By doing so, we can determine the chosen experts ahead of time for each noise level. Figure 2 illustrates this process. This allows us to fuse the selected expert MLPs into a single, composite MLP, effectively reducing the computation cost. Instead of looping through each expert individually, this fused expert MLP can run in parallel, which substantially decreases the overall latency of the network. By eliminating the need for dynamically invoking each expert, we not only save time but also streamline memory access patterns, reducing the overhead typically associated with routing decisions in a traditional MoE setup. Our caching strategy reduces the FLOPs overhead by over 80% compared to standard MoE rollouts and makes it two times faster during inference.

3.4 Generalist Policy Pre-Training

We pretrain MoDE on a diverse mix of multi-robot datasets curated from the OXE dataset Collaboration et al. (2023). Our training data comprises 196k trajectories selected from six diverse datasets, featuring various robot platforms and manipulation tasks. The pretraining process of MoDE runs for 300k steps on a distributed Cluster of 6 GPUs over three days For finetuning we freeze the pretrained routers in each layer and only finetune the other model components. An comprehensive overview of our pretraining mix and used datasets is given in subsubsection A.0.1 in the Appendix. In detailed comparisons presented in subsubsection A.1.1 in the Appendix, MoDE outperforms state-of-the-art generalist policies Octo and OpenVLA, achieving an average success rate of 26.30% across diverse manipulation tasks compared to 23.70% (OpenVLA) and 17.75% (Octo).

4 Evaluation

Our experiments aim to answer four key questions: (I) How does MoDE compare to other policies and prior diffusion transformer architectures in terms of performance? (II) Does large-scale pre-training of diverse robotics data boost the performance of MoDE? (III) What is MoDE's efficiency and speed compared to dense transformer baselines? (IV) Which token routing strategy is most effective for Diffusion Policies in state-based and image-based environments? (V) How does the model utilize different experts during the action-denoising process?

We compare MoDE against prior diffusion transformer architecture (Chi et al., 2023), ensuring fair comparisons by using a similar number of active parameters. MoDE uses 8 layers with 4 experts and a latent dimension of 1024 in all experiments. Our pretrained variant is slightly bigger with 12 layers and 4 experts with the same latent dimension of 1024. We use an action chunking length of 10 and a history length of 1 for all experiments. MoDE does execute all 10 generated actions without early re-planning or temporal aggregation. Detailed hyperparameters are provided in the Appendix (Table 3).

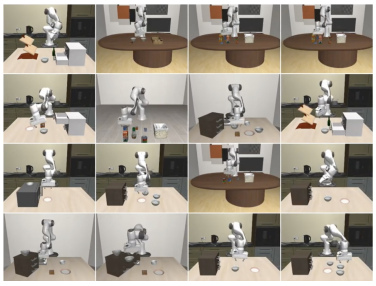

(a) LIBERO-90 Tasks

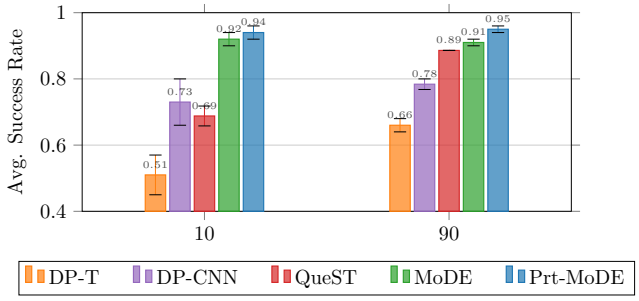

(b) Results for LIBERO-10 and LIBERO-90

Figure 3: Visualization and Results for LIBERO environment. (a) Few example environments and tasks of the LIBERO-90 task suite. (b) Average results for both LIBERO challenges averaged over 3 seeds with 20 rollouts for each task.

4.1 Long-Horizon Multi-Task Experiments

We first evaluate MoDE on the LONG-challenge and LIBERO-90 challenge of the LIBERO benchmark (Liu et al., 2023). The LONG challenge requires a model to learn 10 tasks in different settings. It demands long-horizon behavior generation with several hundreds of steps for completion. The 90 variant tests policies on 90 diverse short-horizon tasks in different environments. Figure 3a visualizes a few examples of these tasks. All environments feature two cameras: a static one and a wrist-mounted camera, used to encode the current observation using FiLM-ResNets-18. We test each policy 20 times on each task and report the average results over 3 seeds. MoDE and all other diffusion architectures use FiLM-conditioned ResNets-18 with a CLIP sentence embedding to encode the goal and the images.

Baselines. We compare MoDE against three state-of-the-art baselines: 1) The Diffusion Transformer (DP-T) architecture (Chi et al., 2023), which conditions on noise and observations using a cross-attention module. 2) The standard Diffusion Policy CNN-based architecture (DP-CNN). 3) QueST (Mete et al., 2024), a transformer-based policy that learns discrete action representations using vector-quantized embeddings of action sequences. We tested all baselines ourselves, except for QueST, whose results are taken directly from their paper.

Results. The performance of all models on the benchmark is summarized in Figure 3b. Overall, MoDE achieves the highest average performance in both benchmarks, while the QueST baseline is the second best in the LIBERO-90 setting and the CNN-architecture is second best in the long horizon setting. These results demonstrate MoDE's ability to learn long-horizon tasks with high accuracy. The performance gap is more pronounced in the challenging LIBERO-10 experiment, where MoDE is the first policy to achieve an over 90% success rate. Furthermore, MoDE surpasses prior best Diffusion baselines by an average of 16% in both settings, all while maintaining its computational advantage. The pretrained MoDE variant achieves an even higher performance in both settings, showing the potential of diverse pretraining. This showcases MoDE's ability to achieve state-of-the-art performance with a more efficient use of computational resources.

4.2 Scaling Multi-Task Experiments

Next, we evaluate MoDE efficacy on the demanding **CALVIN Language-Skills Benchmark** (Mees et al., 2022b), an established image-based benchmark for IL. This benchmark contains a large dataset of human-recorded demonstrations. First, MoDE is tested on the **ABCD→D** challenge, which involves $22,966$ interaction sequences across four environments (A, B, C, D), with each consisting of 64 timesteps and 34 diverse tasks. These tasks require the acquisition of complex, sequential behaviors and the ability to chain together different skills. Figure 4a depicts the diverse configurations of interactive elements within these environments. This particular challenge examines the scaling abilities of policies trained on a rich variety of data and skills across multiple settings. All policies are tested on 1000 instructions chains consisting of 5 tasks in sequence in environment D following the official protocol of CALVIN (Mees et al., 2022b). One example rollout with 5 different tasks is

(a) Environments (b) Example CALVIN-Rollout

Figure 4: Overview of the CALVIN environment. (a) CALVIN contains four different settings (A,B,C,D) with different configurations of slides, drawers and textures. (b) Example rollout consisting of 5 tasks in sequence. The next goal is only given to the policy, if it manages to complete the prior.

Train→Test	Method	Active Params in Million	PrT	No. Instructions in a Row (1000 chains)					
				1	2	3	4	5	**Avg. Len.**
ABCD→D	Diff-P-CNN	321	×	86.3%	72.7%	60.1%	51.2%	41.7%	3.16±0.06
	Diff-P-T	194	×	78.3%	53.9%	33.8%	20.4%	11.3%	1.98±0.09
	RoboFlamingo	1000	✓	96.4%	89.6%	82.4%	74.0%	66.0%	4.09±0.00
	GR-1	130	✓	94.9%	89.6%	84.4%	78.9%	73.1%	4.21±0.00
	MoDE	277	×	96.6%	90.6%	86.6%	80.9%	75.5%	4.30±0.02
	MoDE	436	✓	**97.1%**	**92.5%**	**87.9%**	**83.5%**	**77.9%**	**4.39±0.04**
ABC→D	Diff-P-CNN	321	×	63.5%	35.3%	19.4%	10.7%	6.4%	1.35±0.05
	Diff-P-T	194	×	62.2%	30.9%	13.2%	5.0%	1.6%	1.13±0.02
	RoboFlamingo	1000	✓	82.4%	61.9%	46.6%	33.1%	23.5%	2.47±0.00
	SuSIE	860+	✓	87.0%	69.0%	49.0%	38.0%	26.0%	2.69±0.00
	GR-1	130	✓	85.4%	71.2%	59.6%	49.7%	40.1%	3.06±0.00
	MoDE	307	×	91.5%	79.2%	67.3%	55.8%	45.3%	3.39±0.03
	MoDE	436	✓	**96.7%**	**88.6%**	**80.2%**	**70.7%**	**60.9%**	**3.98±0.04**

Table 1: Performance comparison on the two CALVIN challenges. The table reports average success rates for individual tasks within instruction chains and the average rollout length (Avg. Len.) to complete 5 consecutive instructions, based on 1000 chains. Zero standard deviation indicates methods without reported average performance. "Prt" denotes models requiring policy pretraining. Parameter counts exclude language encoders.

visualized in Figure 4b. In terms of scoring, the model receives 1 point for completing a task and only progresses to the next task upon completion of the prior one. We report the average sequence length over 3 seeds with 1000 instruction chains each.

Baselines. We test MODE against several methods specialized for learning language-conditioned behavior and against other baseline diffusion policy architectures. We also compare MoDE against RoboFlamingo and GR-1. RoboFlamingo is a fine-tuned Vision-Language-Action model, that contains around 3 billion parameters and has been pre-trained on diverse internet data. GR-1 is a generative decoder-only Transformer pretrained on large-scale video generation and then co-finetuned on CALVIN (Wu et al., 2024). If available, we report the average performance of all prior work directly from their paper, given the standard evaluation protocol in CALVIN (Mees et al., 2022a).

Results. Our findings, outlined in Table 1 reveal that MoDE outperforms all other policies in terms of average success rate. Moreover, MoDE without pretraining outperforms well-established baselines like RoboFlamingo and GR-1, which depend on extensive internet-scale pretraining. Our larger pretrained version achieves even higher performance. Notably, while GR-1 uses fewer active parameters (130M compared to MoDE's 277M), it operates with a history length of 10 and 15 tokens for each timestep and uses pretrained ViTs for image embeddings. MoDE proves more computationally efficient, requiring fewer FLOPs during inference (1.53 vs 27.5 GFLOPS for GR-1) and being equally fast although its more than 6 times larger (12.2 vs 12.6 ms). The combination of sota performance and low computational demands positions MoDE as a highly practical solution for multitask settings.

4.3 Zero-shot Generalization Experiments

Finally, we then extend our investigation to the **ABC→D** challenge in the second phase, testing MoDE's zero-shot generalization abilities. In this experiment, models are only trained on data from the first three CALVIN environments A,B,C and tested on the unseen setting of environment D, which has different positions of relevant objects and texture of the table. This requires policies, that are able to generalize their learned behavior to new environment configurations and different textures, which is especially challenging. We evaluate MoDE trained from scratch and MoDE pretrained on a sub-set of Open-X-Embodiment Data. This enables us to study the zero-shot performance and pretraining effectiveness of MoDE.

Baselines. For this experiment, we compare MODE against the previous CALVIN baselines, with the addition of SuSIE (Black et al., 2023). A hierarchical policy utilizing a finetuned image-generation model, Instruct2Pix (Brooks et al., 2023), to generate goal images, which guide a low-level diffusion policy. The high-level goal generation model requires large-scale pretraining. SuSIE's results are based on 100 rollouts only, without standard deviation, due to the computational cost of generating subgoal images.

Results. The results of this experiment are summarized in the lower part of Table 1. MoDE outperforms all tested baselines and surpasses all other Diffusion Policy architectures by a wide margin. Further, by pretraining MoDE on diverse robotics data, we achieve a new sota performance of 3.98. Therefore, in response to Question (I), we affirmatively conclude that Mixture-of-Experts models not only enhance scaling performance but also demonstrate strong zero-shot generalization capabilities. In addition, we can answer Question (II) by concluding that pretraining boost performance in challenging zero-shot settings.

4.4 Computational Efficiency of MoDE

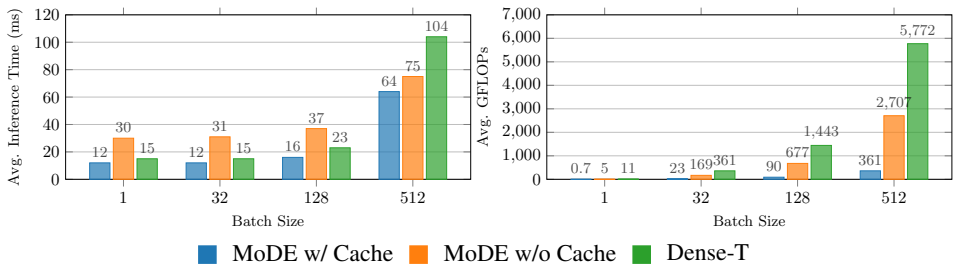

Figure 5: Computational efficiency comparison between MoDE and a Dense-Transformer model with the same number of parameters. Left: Average inference speed over 100 forward passes for various batch sizes. Right: FLOP count for MoDE with router cache and without compared against a dense baseline. MoDE demonstrates superior efficiency with lower FLOP count and faster inference thanks to its router caching and sparse expert design.

We compare MoDE against a dense transformer baseline with similar parameters by measuring average inference time and FLOPs across batch sizes. As shown in Figure Figure 5, MoDE with caching significantly improves computational efficiency - at batch size 1, inference is 20% faster (12ms vs 15ms), while at batch size 512, MoDE requires 16x fewer FLOPs (361 vs 5,772 GFLOPS) and achieves nearly 40% faster inference (64ms vs 104ms). These results demonstrate that MoDE delivers both superior task performance and substantial computational efficiency through its architecture and caching mechanism. A detailed comparison of inference speed and FLOPS against all other baselines on CALVIN is summarized in subsection A.3.

4.5 Ablation Studies

To thoroughly evaluate MoDE's design choices, we conducted a series of ablation studies. These experiments address our research questions: the computational efficiency of MoDE (Question III), the impact of routing strategies (Question IV), and the token distribution (Question V).

4.5.1 WHAT DESIGN DECISIONS AFFECT MODE'S PERFORMANCE?

First, we assess the impact of various design decisions on MoDE's performance. We ablate the choice of noise-conditioning and various MoE strategies on the LIBERO-10 benchmark. The results are summarized in Table 2.

Noise-Injection Ablations. Our experiments reveal the importance of proper noise conditioning in MoDE. The full MoDE model, which uses both input noise tokens and noise-conditioned self-attention, achieves the best performance with an average success rate of 0.92. Removing the input noise token slightly decreases performance to 0.90, highlighting the complementary nature of both conditioning methods. Using only the noise token for conditioning, without noise-conditioned self-attention, further reduces performance to 0.85. Interestingly, using FiLM conditioning (Perez et al., 2018), a common approach in image-diffusion (Peebles & Xie, 2023), yields the lowest performance in this group at 0.81. These results underscore the effectiveness of our proposed noise conditioning strategy in MoDE, demonstrating a clear performance advantage of 0.08 over the FiLM approach.

MoE Ablations. Next, we ablate several design decisions regarding Mixture-of-Experts. First, we test the topk number of used experts. Setting topk to 1 only marginally lowers the average performance from 0.92 to 0.91. MoDE maintains robust performance even with a single expert. We also examine the effect of using a shared expert, where the model consistently employs the same expert in all cases. This approach achieves a comparable average success rate of 0.90. Different choices for the token-distribution loss are also tested. While MoDE uses $\gamma = 0.01$ as a default value, we experiment with γ values of 0.1 and 0.001, which result in average success rates of 0.90 and 0.86, respectively. These results indicate that a γ value of 0.01 strikes the best performance.

	Avg. Success.
MoDE	**0.92**
- Input Noise Token	0.90
- Noise-cond Attention	0.85
FiLM Noise Conditioning	0.81
TopK=1	0.91
Shared Expert	0.90
$\gamma = 0.1$	0.90
$\gamma = 0.001$	0.86
256 Embed Dim	0.86
512 Embed Dim	0.87

Table 2: Ablation Studies for MoDE on LIBERO-10. All results are averaged over 3 seeds with 20 rollouts each.

Latent Dimension. We investigate the impact of varying the latent dimension in MoDE, testing dimensions of 256, 512, and 1024 (our default). The results show that increasing the latent dimension from 256 to 512 yields a modest performance improvement from 0.86 to 0.87, while further increasing to 1024 provides a more substantial boost to 0.92. This suggests that a larger latent dimension allows MoDE to capture more complex representations, leading to improved performance.

4.5.2 OPTIMAL ROUTING STRATEGY FOR DIFFUSION TRANSFORMERS

Next, we answer Question (III) by testing different routing strategies for our diffusion-transformer policy across several environments. We test two different token routing strategies: 1) Token-only conditioned Routing and 2) Noise-only Token Routing. (1) is commonly used in LLMs, where the routing is decided based on the tokens only. We test these strategies in five experiments and report the average performance over 3 seeds: Noise-only Routing achieves an average normalized performance of 0.851, slightly outperforming Token-only Routing, which achieves 0.845. Detailed results are summarized in Table 6 in the Appendix. The results demonstrate the effectiveness of our proposed routing strategy. While the performance difference is small, Noise-only Routing offers an additional advantage: the ability to predict all used experts based on noise levels once before roll-outs, enabling faster inference, as described in subsubsection 3.3.1. This is particularly beneficial for robotics applications.

4.5.3 HOW DOES THE MODEL DISTRIBUTE THE TOKENS TO DIFFERENT EXPERTS?

To address Question IV, we analyzed how MoDE distributes tokens to different experts using a pre-trained model. Figure 6 visualizes the average usage of each expert in each model layer during inference across various noise levels, using 10 denoising steps for clarity. Our analysis reveals that MoDE learns to utilize different experts for various noise levels, suggesting that the router has specialized for different noise regimes. A transition in expert utilization occurs around σ_8. In the first layer, the model learns an expert specialized for low-noise levels, primarily used in the last denoising step at σ_{min}. We conduct more ablations studies with our pretrained model and various other versions

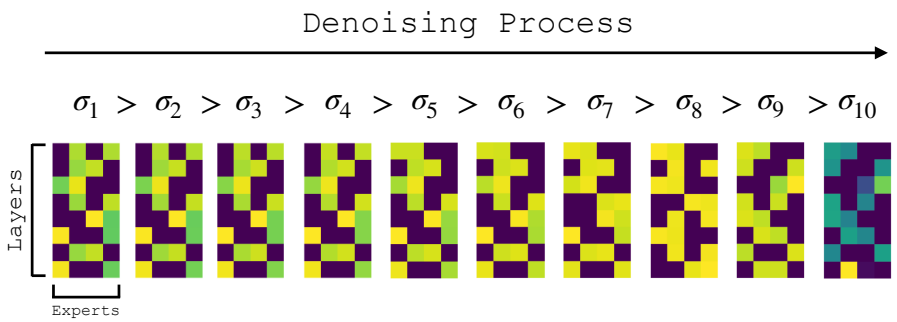

Figure 6: Visualized Expert Utilization. The average usage of all experts in MoDE across all layers is shown. Purple color corresponds to low usage and yellow color to high one, and each image is separately normalized. The average activation shows that MoDE learns to utilize different experts for different noise levels.

of MoDE in subsubsection A.5.1 of the Appendix. These findings affirmatively answer Question IV, demonstrating that MoDE effectively distributes tokens across experts based on noise levels.

4.5.4 How does the model scale with more experts?

Finally, we analyze the effect of increasing the number of experts in MoDE. The results are presented in Figure 8, where we evaluate MoDE on the CALVIN ABCD and CALVIN ABC benchmarks using 2, 4, 6, and 8 experts. For comparison, we include two dense MoDE baselines: Dense-small and Dense-large. Dense-small shares the same latent dimensionality as MoDE, while Dense-large is scaled up to 2024 dimensions, matching MoDE's overall parameter count. Our analysis focuses on how scaling affects both general performance (C-ABCD) and zero-shot generalization (C-ABC). In the ABCD environment, MoDE with 4 experts achieves the best performance. Interestingly, increasing beyond 4 experts degrades performance, possibly due to overfitting or increased routing complexity. In the zero-shot generalization (ABC), MoDE with 4 experts still performs best. Notably, the Dense-small variant consistently underperforms across both tasks, underscoring the efficiency of the MoE architecture in utilizing parameters more effectively. We hypothesize, that 4 experts has an ideal trade-off for the context of noise-only routing of Diffusion Policies. The different expert specialization patterns observed in Figure 6 and Figure 12 from the Appendix show that expert specialization are based on noise regions. MoDE with more than 4 experts does not have a performance benefit. Overall, MoDE demonstrates that it can achieve comparable or superior performance to dense transformer models while requiring fewer computational resources.

4.6 Limitations

MoDE still has certain limitations. In our experiments, we find that MoDE exhibits a slightly higher standard deviation compared to the baselines. We hypothesize that the router's initialization has significant impact on overall optimization, requiring future work on stabilizing routing models. In addition, when visualizing expert utilization, in some of our experiments we noticed that only a subset of the total experts were being utilized - a phenomenon known as expert collapse (Chi et al., 2022).

5 Conclusion

In this work, we introduced Mixture-of-Denoising Experts (MoDE), a novel Diffusion Policy that leverages a mixture of experts Transformer to enhance the performance and efficiency of diffusion policies. We also proposed a noise-conditioned routing strategy for learning specialized experts within our model. In our extensive experiments and ablation studies across diverse benchmarks, we demonstrated the advantages of MoDE to outperform prior Diffusion Policies with a lower number of parameters and 80% less FLOPS during inference. In future work, we want to experiment with more routing strategies, such as expert-choice routing (Zhou et al., 2022).

REFERENCES

Anurag Ajay, Yilun Du, Abhi Gupta, Joshua B. Tenenbaum, Tommi S. Jaakkola, and Pulkit Agrawal. Is conditional generative modeling all you need for decision making? In *International Conference on Learning Representations*, 2023a. URL https://openreview.net/forum?id=sP1fo2K9DFG.

Anurag Ajay, Seungwook Han, Yilun Du, Shaung Li, Abhi Gupta, Tommi Jaakkola, Josh Tenenbaum, Leslie Kaelbling, Akash Srivastava, and Pulkit Agrawal. Compositional foundation models for hierarchical planning. *arXiv preprint arXiv:2309.08587*, 2023b.

Jean-Baptiste Alayrac, Jeff Donahue, Pauline Luc, Antoine Miech, Iain Barr, Yana Hasson, Karel Lenc, Arthur Mensch, Katherine Millican, Malcolm Reynolds, et al. Flamingo: a visual language model for few-shot learning. *Advances in Neural Information Processing Systems*, 35:23716–23736, 2022.

Homanga Bharadhwaj, Jay Vakil, Mohit Sharma, Abhinav Gupta, Shubham Tulsiani, and Vikash Kumar. Roboagent: Generalization and efficiency in robot manipulation via semantic augmentations and action chunking, 2023.

Kevin Black, Mitsuhiko Nakamoto, Pranav Atreya, Homer Walke, Chelsea Finn, Aviral Kumar, and Sergey Levine. Zero-shot robotic manipulation with pretrained image-editing diffusion models. *arXiv preprint arXiv:2310.10639*, 2023.

Denis Blessing, Onur Celik, Xiaogang Jia, Moritz Reuss, Maximilian Xiling Li, Rudolf Lioutikov, and Gerhard Neumann. Information maximizing curriculum: A curriculum-based approach for learning versatile skills. In *Thirty-seventh Conference on Neural Information Processing Systems*, 2023. URL https://openreview.net/forum?id=7eW6NzSE4g.

Anthony Brohan, Noah Brown, Justice Carbajal, Yevgen Chebotar, Joseph Dabis, Chelsea Finn, Keerthana Gopalakrishnan, Karol Hausman, Alex Herzog, Jasmine Hsu, Julian Ibarz, Brian Ichter, Alex Irpan, Tomas Jackson, Sally Jesmonth, Nikhil Joshi, Ryan Julian, Dmitry Kalashnikov, Yuheng Kuang, Isabel Leal, Kuang-Huei Lee, Sergey Levine, Yao Lu, Utsav Malla, Deeksha Manjunath, Igor Mordatch, Ofir Nachum, Carolina Parada, Jodilyn Peralta, Emily Perez, Karl Pertsch, Jornell Quiambao, Kanishka Rao, Michael Ryoo, Grecia Salazar, Pannag Sanketi, Kevin Sayed, Jaspiar Singh, Sumedh Sontakke, Austin Stone, Clayton Tan, Huong Tran, Vincent Vanhoucke, Steve Vega, Quan Vuong, Fei Xia, Ted Xiao, Peng Xu, Sichun Xu, Tianhe Yu, and Brianna Zitkovich. Rt-1: Robotics transformer for real-world control at scale. In *arXiv preprint arXiv:2212.06817*, 2022.

Anthony Brohan, Noah Brown, Justice Carbajal, Yevgen Chebotar, Xi Chen, Krzysztof Choromanski, Tianli Ding, Danny Driess, Avinava Dubey, Chelsea Finn, et al. Rt-2: Vision-language-action models transfer web knowledge to robotic control. *arXiv preprint arXiv:2307.15818*, 2023.

Tim Brooks, Aleksander Holynski, and Alexei A. Efros. Instructpix2pix: Learning to follow image editing instructions. In *CVPR*, 2023.

Joao Carvalho, An T Le, Mark Baierl, Dorothea Koert, and Jan Peters. Motion planning diffusion: Learning and planning of robot motions with diffusion models. In *2023 IEEE/RSJ International Conference on Intelligent Robots and Systems (IROS)*, pp. 1916–1923. IEEE, 2023.

Onur Celik, Dongzhuoran Zhou, Ge Li, Philipp Becker, and Gerhard Neumann. Specializing versatile skill libraries using local mixture of experts. In Aleksandra Faust, David Hsu, and Gerhard Neumann (eds.), *Proceedings of the 5th Conference on Robot Learning*, volume 164 of *Proceedings of Machine Learning Research*, pp. 1423–1433. PMLR, 08–11 Nov 2022. URL https://proceedings.mlr.press/v164/celik22a.html.

Onur Celik, Aleksandar Taranovic, and Gerhard Neumann. Acquiring diverse skills using curriculum reinforcement learning with mixture of experts. *arXiv preprint arXiv:2403.06966*, 2024.

Cheng Chi, Siyuan Feng, Yilun Du, Zhenjia Xu, Eric Cousineau, Benjamin Burchfiel, and Shuran Song. Diffusion policy: Visuomotor policy learning via action diffusion. In *Proceedings of Robotics: Science and Systems (RSS)*, 2023.

Zewen Chi, Li Dong, Shaohan Huang, Damai Dai, Shuming Ma, Barun Patra, Saksham Singhal, Payal Bajaj, Xia Song, Xian-Ling Mao, Heyan Huang, and Furu Wei. On the representation collapse of sparse mixture of experts. In Alice H. Oh, Alekh Agarwal, Danielle Belgrave, and Kyunghyun Cho (eds.), *Advances in Neural Information Processing Systems*, 2022. URL https://openreview.net/forum?id=mWaYC6CZf5.

Open X-Embodiment Collaboration, Abhishek Padalkar, Acorn Pooley, Ajinkya Jain, Alex Bewley, Alex Herzog, Alex Irpan, Alexander Khazatsky, Anant Rai, Anikait Singh, Anthony Brohan, Antonin Raffin, Ayzaan Wahid, Ben Burgess-Limerick, Beomjoon Kim, Bernhard Schölkopf, Brian Ichter, Cewu Lu, Charles Xu, Chelsea Finn, Chenfeng Xu, Cheng Chi, Chenguang Huang, Christine Chan, Chuer Pan, Chuyuan Fu, Coline Devin, Danny Driess, Deepak Pathak, Dhruv Shah, Dieter Büchler, Dmitry Kalashnikov, Dorsa Sadigh, Edward Johns, Federico Ceola, Fei Xia, Freek Stulp, Gaoyue Zhou, Gaurav S. Sukhatme, Gautam Salhotra, Ge Yan, Giulio Schiavi, Hao Su, Hao-Shu Fang, Haochen Shi, Heni Ben Amor, Henrik I Christensen, Hiroki Furuta, Homer Walke, Hongjie Fang, Igor Mordatch, Ilija Radosavovic, Isabel Leal, Jacky Liang, Jaehyung Kim, Jan Schneider, Jasmine Hsu, Jeannette Bohg, Jeffrey Bingham, Jiajun Wu, Jialin Wu, Jianlan Luo, Jiayuan Gu, Jie Tan, Jihoon Oh, Jitendra Malik, Jonathan Tompson, Jonathan Yang, Joseph J. Lim, João Silvério, Junhyek Han, Kanishka Rao, Karl Pertsch, Karol Hausman, Keegan Go, Keerthana Gopalakrishnan, Ken Goldberg, Kendra Byrne, Kenneth Oslund, Kento Kawaharazuka, Kevin Zhang, Keyvan Majd, Krishan Rana, Krishnan Srinivasan, Lawrence Yunliang Chen, Lerrel Pinto, Liam Tan, Lionel Ott, Lisa Lee, Masayoshi Tomizuka, Maximilian Du, Michael Ahn, Mingtong Zhang, Mingyu Ding, Mohan Kumar Srirama, Mohit Sharma, Moo Jin Kim, Naoaki Kanazawa, Nicklas Hansen, Nicolas Heess, Nikhil J Joshi, Niko Suenderhauf, Norman Di Palo, Nur Muhammad Mahi Shafiullah, Oier Mees, Oliver Kroemer, Pannag R Sanketi, Paul Wohlhart, Peng Xu, Pierre Sermanet, Priya Sundaresan, Quan Vuong, Rafael Rafailov, Ran Tian, Ria Doshi, Roberto Martín-Martín, Russell Mendonca, Rutav Shah, Ryan Hoque, Ryan Julian, Samuel Bustamante, Sean Kirmani, Sergey Levine, Sherry Moore, Shikhar Bahl, Shivin Dass, Shuran Song, Sichun Xu, Siddhant Haldar, Simeon Adebola, Simon Guist, Soroush Nasiriany, Stefan Schaal, Stefan Welker, Stephen Tian, Sudeep Dasari, Suneel Belkhale, Takayuki Osa, Tatsuya Harada, Tatsuya Matsushima, Ted Xiao, Tianhe Yu, Tianli Ding, Todor Davchev, Tony Z. Zhao, Travis Armstrong, Trevor Darrell, Vidhi Jain, Vincent Vanhoucke, Wei Zhan, Wenxuan Zhou, Wolfram Burgard, Xi Chen, Xiaolong Wang, Xinghao Zhu, Xuanlin Li, Yao Lu, Yevgen Chebotar, Yifan Zhou, Yifeng Zhu, Ying Xu, Yixuan Wang, Yonatan Bisk, Yoonyoung Cho, Youngwoon Lee, Yuchen Cui, Yueh hua Wu, Yujin Tang, Yuke Zhu, Yunzhu Li, Yusuke Iwasawa, Yutaka Matsuo, Zhuo Xu, and Zichen Jeff Cui. Open X-Embodiment: Robotic learning datasets and RT-X models. https://arxiv.org/abs/2310.08864, 2023.

Zichen Jeff Cui, Yibin Wang, Nur Muhammad Mahi Shafiullah, and Lerrel Pinto. From play to policy: Conditional behavior generation from uncurated robot data. In *International Conference on Learning Representations*, 2023. URL https://openreview.net/forum?id=c7rM7F7jQjN.

Nan Du, Yanping Huang, Andrew M. Dai, Simon Tong, Dmitry Lepikhin, Yuanzhong Xu, Maxim Krikun, Yanqi Zhou, Adams Wei Yu, Orhan Firat, Barret Zoph, Liam Fedus, Maarten Bosma, Zongwei Zhou, Tao Wang, Yu Emma Wang, Kellie Webster, Marie Pellat, Kevin Robinson, Kathleen Meier-Hellstern, Toju Duke, Lucas Dixon, Kun Zhang, Quoc V Le, Yonghui Wu, Zhifeng Chen, and Claire Cui. Glam: Efficient scaling of language models with mixture-of-experts, 2022.

Yilun Du, Mengjiao Yang, Bo Dai, Hanjun Dai, Ofir Nachum, Joshua B Tenenbaum, Dale Schuurmans, and Pieter Abbeel. Learning universal policies via text-guided video generation. *arXiv preprint arXiv:2302.00111*, 2023.

William Fedus, Barret Zoph, and Noam Shazeer. Switch transformers: Scaling to trillion parameter models with simple and efficient sparsity. *Journal of Machine Learning Research*, 23(120):1–39, 2022.

Zipeng Fu, Tony Z Zhao, and Chelsea Finn. Mobile aloha: Learning bimanual mobile manipulation with low-cost whole-body teleoperation. *arXiv preprint arXiv:2401.02117*, 2024.

Hyojun Go, Yunsung Lee, Jin-Young Kim, Seunghyun Lee, Myeongho Jeong, Hyun Seung Lee, and Seungtaek Choi. Towards practical plug-and-play diffusion models. In *Proceedings of the IEEE/CVF conference on computer vision and pattern recognition*, pp. 1962–1971, 2023.

Jiayuan Gu, Sean Kirmani, Paul Wohlhart, Yao Lu, Montserrat Gonzalez Arenas, Kanishka Rao, Wenhao Yu, Chuyuan Fu, Keerthana Gopalakrishnan, Zhuo Xu, Priya Sundaresan, Peng Xu, Hao Su, Karol Hausman, Chelsea Finn, Quan Vuong, and Ted Xiao. Rt-trajectory: Robotic task generalization via hindsight trajectory sketches. In *International Conference on Learning Representations*, 2024.

Tiankai Hang, Shuyang Gu, Chen Li, Jianmin Bao, Dong Chen, Han Hu, Xin Geng, and Baining Guo. Efficient diffusion training via min-snr weighting strategy, 2024.

Kay Hansel, Julen Urain, Jan Peters, and Georgia Chalvatzaki. Hierarchical policy blending as inference for reactive robot control. In *2023 IEEE International Conference on Robotics and Automation (ICRA)*, pp. 10181–10188. IEEE, 2023.

Hussein Hazimeh, Zhe Zhao, Aakanksha Chowdhery, Maheswaran Sathiamoorthy, Yihua Chen, Rahul Mazumder, Lichan Hong, and Ed H. Chi. Dselect-k: Differentiable selection in the mixture of experts with applications to multi-task learning. *CoRR*, abs/2106.03760, 2021. URL https://arxiv.org/abs/2106.03760.

Jonathan Ho, Ajay Jain, and Pieter Abbeel. Denoising diffusion probabilistic models. *Advances in Neural Information Processing Systems*, 33:6840–6851, 2020.

Michael Janner, Yilun Du, Joshua Tenenbaum, and Sergey Levine. Planning with diffusion for flexible behavior synthesis. In *International Conference on Machine Learning*, pp. 9902–9915. PMLR, 2022.

Xiaogang Jia, Denis Blessing, Xinkai Jiang, Moritz Reuss, Atalay Donat, Rudolf Lioutikov, and Gerhard Neumann. Towards diverse behaviors: A benchmark for imitation learning with human demonstrations. In *The Twelfth International Conference on Learning Representations*, 2024. URL https://openreview.net/forum?id=6pPYRXKPpw.

Albert Q Jiang, Alexandre Sablayrolles, Antoine Roux, Arthur Mensch, Blanche Savary, Chris Bamford, Devendra Singh Chaplot, Diego de las Casas, Emma Bou Hanna, Florian Bressand, et al. Mixtral of experts. *arXiv preprint arXiv:2401.04088*, 2024.

Tero Karras, Miika Aittala, Timo Aila, and Samuli Laine. Elucidating the design space of diffusion-based generative models. In Alice H. Oh, Alekh Agarwal, Danielle Belgrave, and Kyunghyun Cho (eds.), *Advances in Neural Information Processing Systems*, 2022.

Tsung-Wei Ke, Nikolaos Gkanatsios, and Katerina Fragkiadaki. 3d diffuser actor: Policy diffusion with 3d scene representations. *arXiv preprint arXiv:2402.10885*, 2024.

Moo Jin Kim, Karl Pertsch, Siddharth Karamcheti, Ted Xiao, Ashwin Balakrishna, Suraj Nair, Rafael Rafailov, Ethan Foster, Grace Lam, Pannag Sanketi, et al. Openvla: An open-source vision-language-action model. *arXiv preprint arXiv:2406.09246*, 2024.

Po-Chen Ko, Jiayuan Mao, Yilun Du, Shao-Hua Sun, and Joshua B Tenenbaum. Learning to Act from Actionless Video through Dense Correspondences. *arXiv:2310.08576*, 2023.

An Thai Le, Kay Hansel, Jan Peters, and Georgia Chalvatzaki. Hierarchical policy blending as optimal transport. In *Learning for Dynamics and Control Conference*, pp. 797–812. PMLR, 2023.

Seungjae Lee, Yibin Wang, Haritheja Etukuru, H. Jin Kim, Nur Muhammad Mahi Shafiullah, and Lerrel Pinto. Behavior generation with latent actions. *arXiv preprint arXiv:2403.03181*, 2024a.

Yunsung Lee, JinYoung Kim, Hyojun Go, Myeongho Jeong, Shinhyeok Oh, and Seungtaek Choi. Multi-architecture multi-expert diffusion models. In *Proceedings of the AAAI Conference on Artificial Intelligence*, volume 38, pp. 13427–13436, 2024b.

Mike Lewis, Shruti Bhosale, Tim Dettmers, Naman Goyal, and Luke Zettlemoyer. Base layers: Simplifying training of large, sparse models, 2021.

Maximilian Xiling Li, Onur Celik, Philipp Becker, Denis Blessing, Rudolf Lioutikov, and Gerhard Neumann. Curriculum-based imitation of versatile skills. In *2023 IEEE International Conference on Robotics and Automation (ICRA)*, pp. 2951–2957, 2023a. doi: 10.1109/ICRA48891.2023.10160543.

Xiang Li, Varun Belagali, Jinghuan Shang, and Michael S Ryoo. Crossway diffusion: Improving diffusion-based visuomotor policy via self-supervised learning. *arXiv preprint arXiv:2307.01849*, 2023b.

Xinghang Li, Minghuan Liu, Hanbo Zhang, Cunjun Yu, Jie Xu, Hongtao Wu, Chilam Cheang, Ya Jing, Weinan Zhang, Huaping Liu, et al. Vision-language foundation models as effective robot imitators. In *International Conference on Learning Representations*, 2024a.

Xuanlin Li, Kyle Hsu, Jiayuan Gu, Karl Pertsch, Oier Mees, Homer Rich Walke, Chuyuan Fu, Ishikaa Lunawat, Isabel Sieh, Sean Kirmani, Sergey Levine, Jiajun Wu, Chelsea Finn, Hao Su, Quan Vuong, and Ted Xiao. Evaluating real-world robot manipulation policies in simulation. *arXiv preprint arXiv:2405.05941*, 2024b.

Bo Liu, Yifeng Zhu, Chongkai Gao, Yihao Feng, Qiang Liu, Yuke Zhu, and Peter Stone. Libero: Benchmarking knowledge transfer for lifelong robot learning. *arXiv preprint arXiv:2306.03310*, 2023.

Corey Lynch, Mohi Khansari, Ted Xiao, Vikash Kumar, Jonathan Tompson, Sergey Levine, and Pierre Sermanet. Learning latent plans from play, 2019.

Oier Mees, Andreas Eitel, and Wolfram Burgard. Choosing smartly: Adaptive multimodal fusion for object detection in changing environments. In *2016 IEEE/RSJ International Conference on Intelligent Robots and Systems (IROS)*, pp. 151–156. IEEE, 2016.

Oier Mees, Lukas Hermann, and Wolfram Burgard. What matters in language conditioned robotic imitation learning over unstructured data. *IEEE Robotics and Automation Letters (RA-L)*, 7(4): 11205–11212, 2022a.

Oier Mees, Lukas Hermann, Erick Rosete-Beas, and Wolfram Burgard. Calvin: A benchmark for language-conditioned policy learning for long-horizon robot manipulation tasks. *IEEE Robotics and Automation Letters*, 2022b.

Atharva Mete, Haotian Xue, Albert Wilcox, Yongxin Chen, and Animesh Garg. Quest: Self-supervised skill abstractions for learning continuous control. *arXiv preprint arXiv:2407.15840*, 2024.

Ashvin Nair, Dian Chen, Pulkit Agrawal, Phillip Isola, Pieter Abbeel, Jitendra Malik, and Sergey Levine. Combining self-supervised learning and imitation for vision-based rope manipulation. In *2017 IEEE international conference on robotics and automation (ICRA)*, pp. 2146–2153. IEEE, 2017.

Johan Obando-Ceron, Ghada Sokar, Timon Willi, Clare Lyle, Jesse Farebrother, Jakob Foerster, Gintare Karolina Dziugaite, Doina Precup, and Pablo Samuel Castro. Mixtures of experts unlock parameter scaling for deep rl. *arXiv preprint arXiv:2402.08609*, 2024.

Octo Model Team, Dibya Ghosh, Homer Walke, Karl Pertsch, Kevin Black, Oier Mees, Sudeep Dasari, Joey Hejna, Charles Xu, Jianlan Luo, Tobias Kreiman, You Liang Tan, Dorsa Sadigh, Chelsea Finn, and Sergey Levine. Octo: An open-source generalist robot policy. `https://octo-models.github.io`, 2023.

Jyothish Pari, Nur Muhammad Shafiullah, Sridhar Pandian Arunachalam, and Lerrel Pinto. The surprising effectiveness of representation learning for visual imitation, 2021.

Jyothish Pari, Nur Muhammad (Mahi) Shafiullah, Sridhar Pandian Arunachalam, and Lerrel Pinto. The Surprising Effectiveness of Representation Learning for Visual Imitation. In *Proceedings of Robotics: Science and Systems*, New York City, NY, USA, June 2022. doi: 10.15607/RSS.2022.XVIII.010.

Byeongjun Park, Sangmin Woo, Hyojun Go, Jin-Young Kim, and Changick Kim. Denoising task routing for diffusion models. *arXiv preprint arXiv:2310.07138*, 2023.

Byeongjun Park, Hyojun Go, Jin-Young Kim, Sangmin Woo, Seokil Ham, and Changick Kim. Switch diffusion transformer: Synergizing denoising tasks with sparse mixture-of-experts. *arXiv preprint arXiv:2403.09176*, 2024.

William Peebles and Saining Xie. Scalable diffusion models with transformers. In *Proceedings of the IEEE/CVF International Conference on Computer Vision*, pp. 4195–4205, 2023.

Ethan Perez, Florian Strub, Harm De Vries, Vincent Dumoulin, and Aaron Courville. Film: Visual reasoning with a general conditioning layer. In *Proceedings of the AAAI conference on artificial intelligence*, volume 32, 2018.

Dean Pomerleau. Alvinn: An autonomous land vehicle in a neural network. In D.S. Touretzky (ed.), *Proceedings of (NeurIPS) Neural Information Processing Systems*, pp. 305 – 313. Morgan Kaufmann, December 1989.

Moritz Reuss, Maximilian Li, Xiaogang Jia, and Rudolf Lioutikov. Goal conditioned imitation learning using score-based diffusion policies. In *Proceedings of Robotics: Science and Systems (RSS)*, 2023.

Carlos Riquelme, Joan Puigcerver, Basil Mustafa, Maxim Neumann, Rodolphe Jenatton, André Susano Pinto, Daniel Keysers, and Neil Houlsby. Scaling vision with sparse mixture of experts, 2021.

Stephen Roller, Sainbayar Sukhbaatar, Arthur Szlam, and Jason Weston. Hash layers for large sparse models. *CoRR*, abs/2106.04426, 2021. URL https://arxiv.org/abs/2106.04426.

Paul Maria Scheikl, Nicolas Schreiber, Christoph Haas, Niklas Freymuth, Gerhard Neumann, Rudolf Lioutikov, and Franziska Mathis-Ullrich. Movement primitive diffusion: Learning gentle robotic manipulation of deformable objects. *arXiv preprint arXiv:2312.10008*, 2023.

Nur Muhammad Mahi Shafiullah, Zichen Jeff Cui, Ariuntuya Altanzaya, and Lerrel Pinto. Behavior transformers: Cloning k modes with one stone. In *Thirty-Sixth Conference on Neural Information Processing Systems*, 2022. URL https://openreview.net/forum?id=agTr-vRQsa.

Noam Shazeer, Azalia Mirhoseini, Krzysztof Maziarz, Andy Davis, Quoc Le, Geoffrey Hinton, and Jeff Dean. Outrageously large neural networks: The sparsely-gated mixture-of-experts layer, 2017.

Jiaming Song, Chenlin Meng, and Stefano Ermon. Denoising diffusion implicit models. In *ICLR*, 2021.

Yang Song and Stefano Ermon. Generative modeling by estimating gradients of the data distribution. *Advances in Neural Information Processing Systems*, 32, 2019.

Yang Song, Jascha Sohl-Dickstein, Diederik P Kingma, Abhishek Kumar, Stefano Ermon, and Ben Poole. Score-based generative modeling through stochastic differential equations. In *International Conference on Learning Representations*, 2020.

Hugo Touvron, Thibaut Lavril, Gautier Izacard, Xavier Martinet, Marie-Anne Lachaux, Timothée Lacroix, Baptiste Rozière, Naman Goyal, Eric Hambro, Faisal Azhar, et al. Llama: Open and efficient foundation language models. *arXiv preprint arXiv:2302.13971*, 2023.

Julen Urain, Niklas Funk, Jan Peters, and Georgia Chalvatzaki. Se (3)-diffusionfields: Learning smooth cost functions for joint grasp and motion optimization through diffusion. In *2023 IEEE International Conference on Robotics and Automation (ICRA)*, pp. 5923–5930. IEEE, 2023.

Ashish Vaswani, Noam Shazeer, Niki Parmar, Jakob Uszkoreit, Llion Jones, Aidan N Gomez, Łukasz Kaiser, and Illia Polosukhin. Attention is all you need. *Advances in neural information processing systems*, 30, 2017.

Pascal Vincent. A connection between score matching and denoising autoencoders. *Neural Computation*, 23(7):1661–1674, 2011. doi: 10.1162/NECO_a_00142.

Homer Rich Walke, Kevin Black, Tony Z Zhao, Quan Vuong, Chongyi Zheng, Philippe Hansen-Estruch, Andre Wang He, Vivek Myers, Moo Jin Kim, Max Du, et al. Bridgedata v2: A dataset for robot learning at scale. In *Conference on Robot Learning*, pp. 1723–1736. PMLR, 2023.

Tsun-Hsuan Wang, Juntian Zheng, Pingchuan Ma, Yilun Du, Byungchul Kim, Andrew Everett Spielberg, Joshua B. Tenenbaum, Chuang Gan, and Daniela Rus. Diffusebot: Breeding soft robots with physics-augmented generative diffusion models. In *Thirty-seventh Conference on Neural Information Processing Systems*, 2023. URL https://openreview.net/forum?id=1zo4iioUEs.

Hongtao Wu, Ya Jing, Chilam Cheang, Guangzeng Chen, Jiafeng Xu, Xinghang Li, Minghuan Liu, Hang Li, and Tao Kong. Unleashing large-scale video generative pre-training for visual robot manipulation. In *International Conference on Learning Representations*, 2024.

Zhou Xian, Nikolaos Gkanatsios, Theophile Gervet, Tsung-Wei Ke, and Katerina Fragkiadaki. Chaineddiffuser: Unifying trajectory diffusion and keypose prediction for robotic manipulation. In *7th Annual Conference on Robot Learning*, 2023. URL https://openreview.net/forum?id=W0zgY2mBTA8.

Tony Z Zhao, Vikash Kumar, Sergey Levine, and Chelsea Finn. Learning fine-grained bimanual manipulation with low-cost hardware. *arXiv preprint arXiv:2304.13705*, 2023.

Yanqi Zhou, Tao Lei, Hanxiao Liu, Nan Du, Yanping Huang, Vincent Zhao, Andrew Dai, Zhifeng Chen, Quoc Le, and James Laudon. Mixture-of-experts with expert choice routing, 2022.

Brianna Zitkovich, Tianhe Yu, Sichun Xu, Peng Xu, Ted Xiao, Fei Xia, Jialin Wu, Paul Wohlhart, Stefan Welker, Ayzaan Wahid, Quan Vuong, Vincent Vanhoucke, Huong Tran, Radu Soricut, Anikait Singh, Jaspiar Singh, Pierre Sermanet, Pannag R Sanketi, Grecia Salazar, Michael S Ryoo, Krista Reymann, Kanishka Rao, Karl Pertsch, Igor Mordatch, Henryk Michalewski, Yao Lu, Sergey Levine, Lisa Lee, Tsang-Wei Edward Lee, Isabel Leal, Yuheng Kuang, Dmitry Kalashnikov, Ryan Julian, Nikhil J Joshi, Alex Irpan, brian ichter, Jasmine Hsu, Alexander Herzog, Karol Hausman, Keerthana Gopalakrishnan, Chuyuan Fu, Pete Florence, Chelsea Finn, Kumar Avinava Dubey, Danny Driess, Tianli Ding, Krzysztof Marcin Choromanski, Xi Chen, Yevgen Chebotar, Justice Carbajal, Noah Brown, Anthony Brohan, Montserrat Gonzalez Arenas, and Kehang Han. RT-2: Vision-language-action models transfer web knowledge to robotic control. In *7th Annual Conference on Robot Learning*, 2023. URL https://openreview.net/forum?id=XMQgwiJ7KSX.

A APPENDIX / SUPPLEMENTAL MATERIAL

Hyperparameter	CALVIN ABCD	CALVIN ABC	LIBERO-10	LIBERO-90	Pret-MoDE
Number of Transformer Layers	8	8	8	8	12
Number Experts	4	4	4	4	4
Attention Heads	8	8	8	8	8
Action Chunk Size	10	10	10	10	10
History Length	1	1	1	1	1
Embedding Dimension	1024	1024	1024	1024	1024
Image Encoder	FiLM-ResNet18	FiLM-ResNet50	FiLM-ResNet18	FiLM-ResNet18	FiLM-ResNet50
Goal Lang Encoder	CLIP ViT-B/32	CLIP ViT-B/32	CLIP ViT-B/32	CLIP ViT-B/32	CLIP ViT-B/32
Attention Dropout	0.3	0.3	0.3	0.3	0.3
Residual Dropout	0.1	0.1	0.1	0.1	0.1
MLP Dropout	0.1	0.1	0.1	0.1	0.1
Optimizer	AdamW	AdamW	AdamW	AdamW	AdamW
Betas	[0.9, 0.95]	[0.9, 0.95]	[0.9, 0.95]	[0.9, 0.95]	[0.9, 0.95]
Learning Rate	1e-4	1e-4	1e-4	1e-4	1e-4
Transformer Weight Decay	0.05	0.05	0.05	0.05	0.1
Other weight decay	0.05	0.05	0.05	0.05	0.1
Batch Size	512	512	512	512	512
Train Steps in Thousands	30	25	15	30	300
σ_{max}	80	80	80	80	80
σ_{min}	0.001	0.001	0.001	0.001	0.001
σ_t	0.5	0.5	0.5	0.5	0.5
EMA	True	True	True	True	True
Time steps	Exponential	Exponential	Exponential	Exponential	Exponential
Sampler	DDIM	DDIM	DDIM	DDIM	DDIM
Parameter Count (Millions)	460	460	460	460	685

Table 3: Summary of all the Hyperparameters for the MoDE policy used in our experiments.

A.0.1 PRETRAINING DETAILS

Dataset	**Weight**
BC-Z	0.258768
LIBERO-10	0.043649
BRIDGE	0.188043
CMU Play-Fusion	0.101486
Google Fractal	0.162878
DOBB-E	0.245176
Total	1.000000

Table 4: Dataset sampling weights used for training MoDE on a small subset of trajectories. The total dataset consists of 196k trajectories.

We pretrain a large variant of MoDE on a subset of available datasets from the Open-X-Embodiment Collaboration et al. (2023) to study the generalization ability of MoDE. An Overview of the used dataset is summarized in Table 4. Our pretraining dataset comprises 196K trajectories from 6 different sources, with weighted sampling across BC-Z (0.259), LIBERO-10 (0.044), BRIDGE (0.188), CMU Play-Fusion (0.101), Google Fractal (0.163), and DOBB-E (0.245). This dataset includes demonstrations from diverse robot platforms including Google robots, Franka Pandas, and Hello-Stretch robots, covering a wide range of manipulation tasks. The pretraining was conducted on 6 NVIDIA A6000 GPUs with 40GB VRAM each over 3 days, completing 300K training steps. We used a batch size of 1024 with a learning rate of 1e-4 and weight decay of 0.1. To ensure balanced dataset mixing during training, we implemented a large shuffle buffer of 400K samples. Each dataset was individually normalized to account for different scales and ranges across the various robot platforms. This diverse pretraining significantly improved MoDE's zero-shot generalization, particularly on challenging benchmarks like CALVIN ABC→D where we achieved a new state-of-the-art performance of 3.98 average rollout length. For reproducibility, we will release our pretrained model weights and preprocessing code to the community.

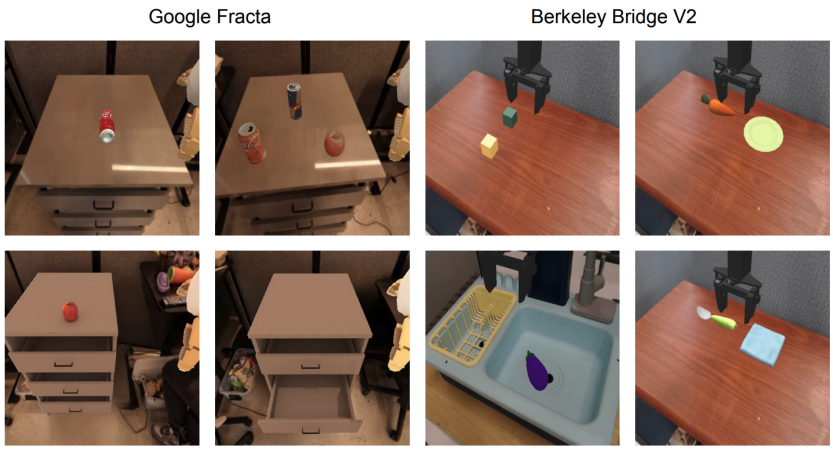

Figure 7: Example Scenes of the SIMPLER Li et al. (2024b) benchmark used to test generalist policies on various tasks from the Bridge and Google Fractal dataset.

For finetuning we freeze the routers of the model and remove the load-balancing loss and train on the local domain for 10k steps on LIBERO and 15k steps for CALVIN with a batch size of 64 per GPU and 4 GPUs.

A.1 Experiments Details

A.1.1 MoDE Evaluation on SIMPLER

We evaluate MoDE's capabilities as a generalist policy by comparing it against two state-of-the-art models trained on substantially larger datasets from Open-X-Embodiment: Octo (800K trajectories) Octo Model Team et al. (2023) and OpenVLA Kim et al. (2024)(1M trajectories). We conduct this comparison using the SIMPLER benchmark, which provides real2sim variants of the Bridge2 Walke et al. (2023) and Google Fractal datasets used to train RT-1 Brohan et al. (2023). The benchmark encompasses diverse manipulation tasks across multiple environments, as illustrated in Figure 7.

The results of the evaluations are summarized in Table 5. On average MoDE achieves the highest average success rate of 26.30% and the best average ranking of 1.65 across all tasks, surpassing both Octo (17.75% success, 2.1 rank) and the 7.7B parameter OpenVLA model (23.70% success, 1.95 rank). MoDE shows particularly strong performance on challenging manipulation tasks like drawer manipulation (34.92% on drawer close) and precise object interactions (40% on vertical can picking). While specialized tasks like stacking blocks remain challenging for all models, MoDE's consistent performance across diverse tasks demonstrates its effectiveness as a scalable architecture for generalist policies.

A.1.2 CALVIN Benchmark

The CALVIN benchmark (Mees et al., 2022b) is an established IL benchmark for learning language-conditioned behavior from human play data. In contrast to other benchmarks the data does not contain structured demonstrations, where the robot completes one task, but instead, the dataset was collected by humans, that randomly interact with the environment. From these long-horizon trajectories across the 4 different settings, the authors randomly cut out short sequences with 64 frames and labeled them with the task label. While the dataset offers models to train on the unlabeled part too, we restricted MoDE to only train on the labeled parts. The Franke Emika Panda robot is controlled using a Delta-End-Effector Space with a discrete gripper. We use two cameras to encode the current scene: a static camera and a wrist one and predict the next 10 actions, before receiving the next observations and generating another set of 10 actions.

CALVIN ABC. We train MoDE and our dense transformer baseline for 25k training steps with a batch size of 512 on a 4 GPU Cluster Node with 4 A6000 NVIDIA GPUs for 6.5 hours with all

Metric	OpenVLA Score	OpenVLA Rank	Octo Base Score	Octo Base Rank	MoDe (ours) Score	MoDe (ours) Rank
Drawer Open	**16%**	**1**	0%	3	4.23%	2
Drawer Close	20%	2	2%	3	**34.92%**	**1**
Pick Can Horizontal	**71%**	**1**	0%	3	33.78%	2
Pick Can Vertical	27%	2	0%	3	**29.78%**	**1**
Pick Can Standing	**65%**	**1**	0%	3	36.44%	2
Move Near	**48%**	**1**	3%	3	30%	2
Drawer Open	19%	2	1%	3	**21.30%**	**1**
Drawer Close	52%	2	44%	3	**76.85%**	**1**
Pick Can Horizontal	**27%**	**1**	21%	3	22%	2
Pick Can Vertical	3%	3	21%	2	**40%**	**1**
Pick Can Standing	19%	2	9%	3	**35%**	**1**
Move Near	**46%**	**1**	4%	3	45.42%	2
Partial Put Spoon on Tablecloth	4%	3	**35%**	**1**	29.17%	2
Put Spoon on Tablecloth	0%	3	12%	**1**	**12.5%**	**1**
Partial Put Carrot on Plate	33%	2	**53%**	**1**	29.17%	3
Put Carrot on Plate	0%	3	8%	**1**	**8.33%**	1
Partial Stack Green Block on Yellow Block	12%	2	**32%**	**1**	8.33%	3
Stack Green Block on Yellow Block	0%	2	0%	2	0%	2
Partial Put Eggplant in Basket	8%	3	**67%**	**1**	37.5%	2
Put Eggplant in Basket	4%	3	**43%**	**1**	8.33%	2
Average	23.70%	1.95	17.75%	2.1	**26.30%**	**1.65**

Table 5: Detailed comparison of MoDE against two sota Generalist Policies OpenVLA Kim et al. (2024) and Octo Octo Model Team et al. (2023) tested on all SIMPLER tasks with 2952 evals.

1000 rollouts at the end of training. We report the mean results averaged over 3 seeds as done in all relevant prior work. All baselines are reported from the original paper given the standardized evaluation protocol of CALVIN (Mees et al., 2022b).

CALVIN ABCD. We train MoDE and our dense transformer baseline for 30k training steps with a batch size of 512 on a 4 GPU Cluster Node with 4 A6000 NVIDIA GPUs for 7.5 hours with all 1000 rollouts at the end of training. We report the mean results averaged over 3 seeds as done in all relevant prior work.

A.1.3 LIBERO BENCHMARK

LIBERO-10. The LIBERO-10 benchmark consists of 50 demonstrations for 10 different tasks that are all labeled with a text instruction. The Franka Emika Panda robot is controlled using an end-effector controller. Similar to CALVIN all models have access to two camera inputs: a static one and a wrist camera. We train MoDE and our dense transformer baseline for 50 epochs with a batch size of 512 on a 4 GPU Cluster Node with 4 A6000 NVIDIA GPUs for 2 hours with all 200 rollouts at the end of training. The benchmark does require to test models on 10 different long-horizon tasks. We test each task 20 times for each model and report the final average performance overall 10 tasks.

LIBERO-90. The LIBERO-10 benchmark consists of 50 demonstrations for 90 different tasks that are all labeled with a text instruction. The Franka Emika Panda robot is controlled using an end-effector controller. We train MoDE and our dense transformer baseline for $50k$ steps with a batch size of 512 on a 4 GPU Cluster Node with 4 A6000 NVIDIA GPUs for 12 hours with all 1800 rollouts at the end of training. The benchmark does require to test models on 90 different tasks in many different environments. We test each task 20 times for each model and report the final average performance overall 90 tasks.

A.2 BASELINES

Below we explain several baselines used in the experiments in detail:

Model	Block Push	Relay Kitchen	CAL ABC	CAL ABCD	L-10	Average
Dense T	0.96±0.02	3.73±0.12	**2.83±0.19**	4.13±0.11	0.91±0.02	0.839±0.144
Token-Router	0.97±0.01	**3.85±0.03**	2.67±0.04	4.29±0.08	0.90±0.01	0.845±0.161
σ_t-Router	*0.97±0.01*	3.79±0.04	*2.79±0.16*	**4.30±0.02**	**0.92±0.02**	**0.851±0.151**

Table 6: Overview of the performance of all different token routing strategies used for MoDE across 5 benchmarks. We mark the best result for each environment in **bold** and the second best in *cursive*. We use CAL to represent CALVIN. To average the results, we normalize all scores and compute the average over all environments.

Method	Active Params (M)	Total Params (M)	GFLOPS	PrT	Avg. Length	SF-Ratio	Inf. Time [ms]
Diff-P-CNN	321	321	1.28	×	1.35	1.05	**11.7**
Diff-P-T	194	194	2.16	×	1.13	0.53	16.2
RoboFlamingo	1000	1000	690	✓	2.47	0.004	65
SuSIE	860+	860+	60	✓	2.69	0.045	199
GR-1	**130**	**130**	27.5	✓	3.06	0.11	12.6
MoDE (ours)	436	740	1.53	✓	**3.98**	**2.6**	12.2

Table 7: Comparison of total and active number of parameters of methods used in the CALVIN benchmark. Additional overview of average FLOPS required by the different methods together with their average performance on the ABC benchmark. SF-Ratio compares average rollout length with GFLOPS.

Diffusion Policy-CNN/T Inspired by (Chi et al., 2023), we evaluate extension of the DDPM based Diffusion Policy framework for goal-conditioned Multi-task learning. We evaluate two versions: the CNN-based variant and the Diffusion-Transformer variant, that is conditioned on context and noise using cross-attention. For our experiments we also use EDM-based Diffusion framework for fair comparison against MoDE. We optimized the ideal number of layers and latent dimension for the Transformer baseline and our final version uses 8 layers with a latent dimension of 1024. Larger or smaller variants resulted in lower average performance.

RoboFlamingo. RoboFlamingo (Li et al., 2024a) is a Vision-Language-Models (VLM) finetuned for behavior generation. The authors use a 3 billion parameter Flamingo model (Alayrac et al., 2022) and fine-tune it on CALVIN by freezing the forward blocks and only fine-tuning a new Perceiver Resampler module to extract features from a frozen vision-transformer image encoder and the cross-attention layers to process the image features. Finally, a new action head is learned to generate actions. Overall, the finetuning requires training approx. 1 billion of the parameters. We report the reported results from the paper since they use the standard CALVIN evaluation suite.

SuSIE. This model first finetunes Instruct2Pix, an image-generation diffusion model, that generates images conditioned on another image and a text description (Brooks et al., 2023) on the local CALVIN robotics domain and uses it as a high-level goal generator. The low-level policy is a CNN-based Diffusion Policy, that predicts the next 4 actions given the current state embedding and desired sub-goal from the high-level policy (Black et al., 2023).

GR-1 A causal GPT-Transformer model (Wu et al., 2024), that has been pretrained on large-scale generative video prediction of human videos. Later, the model is finetuned using co-training of action prediction and video prediction on CALVIN. We report the results directly from their paper for the CALVIN benchmark.

A.3 Average FLOPs computation and Inference Speed

We provide an in-depth comparison of the total parameters and FLOPs used for every method in Table 7. Additionally, we provide the computational efficiency metric per GFLOPS (10^9 FLOPS) to compare the various methods and measure the average prediction time for a single action. In the following, we detail the average GFLOPS computation for all relevant baselines on the CALVIN ABC benchmark. Specifically, we compare the average GFLOPS required to predict a single action.

To guarantee a fair comparison we evaluated all methods on the same NVIDIA A6000 GPU with 40 GB VRAM. To compute the average inference speed, we tested each method 100 times and removed large outliers to compute an average time.

MoDE. We benchmark the large pretrained variant with 12 layers, 4 experts and a hidden dim of 1024. The average GFLOPS for a forward pass are 0.7 GFLOPS. Without router caching, the model would require 5 GFLOPS, indicating that the router caching reduces the overall computational cost by over 80%. The architecture processes 14 tokens in total (1 noise + 1 goal + 2 images + 10 noisy action actions). MoDE predicts a sequence of 10 actions with 10 denoising passes. For the variant with ResNet-50, the image encoder requires 8.27 GFLOPS . On average for a single action, MoDE requires 10 forward passes with the transformer and a single pass with the ResNet-50. Consequently, the pretrained variant of MoDE needs 1.53 GFLOPS on average to predict a single action. The inference time for that model depends on the hardware. We measure an average inference time per action of 12.2.

DP-CNN/T. DP-CNN utilizes 0.8 GFLOPS for an average forward pass. The ResNet-18s require 3.62 GFLOPS. The model predicts 10 actions with 10 denoising steps and executes 10 actions without replanning. This results in the CNN version requiring 1.28 GFLOPS to predict a single action. For the Transformer version, the architecture predicts 10 actions using 10 denoising steps and processes 14 tokens in total (1 noise + 1 goal + 2 images + 10 noisy action actions) similar to MoDE. It achieves an average GFLOPS usage of 1.8 GFLOPS per forward pass through the transformer. The DP-T baseline requires 2.16 GFLOPS on average to predict a single action. The CNN version requires 11.7 ms to predict a single action on average and the transformer variant with its cross-attention conditioning needs 16.2 ms.

RoboFlamingo. For computational analysis, the model requires 34 GFLOPS to encode a single image with a ViT. For the policy backbone, we evaluated the "mpt-1b-redpajama-200b-dolly" variant as used in the paper. This architecture requires 656 GFLOPS for an average sequence of 32 tokens per forward pass. While multiple variants of RoboFlamingo exist, this provides a rough estimate of the required GFLOPS. In total, we estimate an average of 690 GFLOPS to predict an action in CALVIN. To predict a single action, the model requires 65 ms on average.

SuSIE. In our computational analysis, we tested Instruct2Pix with 50 denoising steps as implemented by SuSIE. The resulting 1026 GFLOPS are divided by 20 as the model only generates new subgoals every 20 timesteps. The low-level policy uses a ResNet-50 image encoder with 8.27 GFLOPS. Contrast to other policies, SuSIe only computes one image per state and predicts actions every timestep. These are then averaged using exponential averaging. Thus, we omit the small diffusion head to get an estimate of 60 GFLOPS per action. For the average inference speed we meassure the time to generate a single goal image and divide it by 20, next we add the average time to encode two images with the ResNet-50 and 10 forward passes through a small MLP. Every 20 timesteps, when SuSIE generates a new image it requires 3777.62 ms for a single action generation. Otherwise its a lot faster with 10.7 ms. On average SuSIE requires 199 ms to generate a single action, which make it the slowest policy overall.

GR-1. The pretrained MAE Vision Transformer requires approx. 17.5 GFLOPS to encode a single image. The transformer backbone processes 150 tokens with a history length of 10 and 15 tokens per timestep (10 image tokens + 1 goal token + 1 proprioceptive token + 2 video readout tokens + 1 action token per timestep). Consequently, the average GFLOPS for a single action prediction utilizing the decoder with a latent dimension of 384 and 12 layers are 10 GFLOPS. In total, this results in an average computational cost of 27.5 for predicting a single action in CALVIN. For the average single action prediction the model requires 12.6 ms.

Analysis. Overall, MoDE offers the best performance to GFLOPS ratio across all tested baselines. Although MoDE is significantly larger in total size compared to the other Diffusion Policy architectures it requires similar inference speed and a low FLOP count. Additionally, it has demonstrated superior efficiency in terms of computational resources while maintaining high performance on the CALVIN benchmark tasks. For inference speed MoDE is the second fastest although it has a high total parameter count.

A.4 Detailed Experimental Results

We summarize the ablations regarding the choice of routing in Table 6. Therefore, we test two 2 different routing strategies across 5 benchmarks.

A.5 State-based Experiments

We conduct additional experiments with MoDE on two established multi-task state-based environments:

Relay Kitchen. We utilize the Franka Kitchen environment from (Lynch et al., 2019) to evaluate models. This virtual kitchen environment allows human participants to manipulate seven objects using a VR interface: a kettle, a microwave, a sliding door, a hinged door, a light switch, and two burners. The resulting dataset consists of 566 demonstrations collected by the original researchers, where each participant performed four predetermined manipulation tasks per episode. The Franka Emika Panda robot is controlled via a 9-dimensional action space representing the robot's joint and end-effector positions. The 30-dimensional observation space contains information about the current state of the relevant objects in the environment. As a desired goal state, we randomly sample future states as a desired goal to reach.

For this experiment, we train all models for 40k training steps with a batch size of 1024 and evaluate them 100 times as done in prior work (Shafiullah et al., 2022; Cui et al., 2023; Reuss et al., 2023) to guarantee a fair evaluation. All reported results are averaged over 4 seeds. We train our models on a local PC RTX with an RTX 3070 GPU for approx. 2 hours for each run with the additional experimental rollouts.

Block Push. The PyBullet environment features an XArm robot tasked with pushing two blocks into two square targets within a plane. The desired order of pushing the blocks and the specific block-target combinations are sampled from the set of 1000 demonstrations as a desired goal state. The demonstrations used for training our models were collected using a hard-coded controller that selects a block to push first and independently chooses a target for that block. After pushing the first block to a target, the controller pushes the second block to the remaining target. This approach results in four possible modes of behavior, with additional stochasticity arising from the various ways of pushing a block into a target. The models only get a credit, if the blocks have been pushed in the correct target position and order. We consider a block successfully pushed if its center is within 0.05 units of a target square.

All models were trained on a dataset of 1000 controller-generated demonstrations under these randomized conditions. All models have been trained for 60k steps with a batch size of 1024. To evaluate them we follow prior work (Shafiullah et al., 2022; Cui et al., 2023; Reuss et al., 2023) and test them on 100 different instructions and report the average result over 4 seeds. We train our models on a local PC RTX 3070 GPU for approx. 3 hours for each run with a final evaluation. Demonstrations are sourced from a scripted oracle, which first pushes a randomly chosen block to a selected square, followed by the other block to a different square. The policies are conditioned to push the blocks in the desired configuration using a goal state-vector. We chose an action sequence length of 1 given a history length of 4 for these experiments, which are inspired by our dense diffusion transformer baseline BESO (Reuss et al., 2023).

	Block Push	Relay Kitchen
C-BeT	0.87±(0.07)	3.09±(0.12)
VQ-BeT	0.87±(0.02)	3.78±(0.04)
BESO	0.96±(0.02)	3.73±(0.05)
MoDE	**0.97**±(**0.01**)	**3.79**±(**0.02**)

Table 8: Comparison of the performance of different policies on the state-based goal-conditioned relay-kitchen and block-push environment averaged over 4 seeds. MoDE outperforms the dense transformer variant BESO and other policy representations on all baselines.

Baselines. In this setting, we compare MoDE against several SOTA goal-conditioned policies. We test two transformer architectures, C-BeT (Cui et al., 2023) and VQ-BeT (Lee et al., 2024a), that predict discretized actions with an offset. C-BeT uses k-means clustering together with an offset vector while VQ-BeT leverages residual Vector Quantization to embed actions into a hierarchical latent space. Further, we test against a dense diffusion policy transformer model BESO (Reuss et al.,

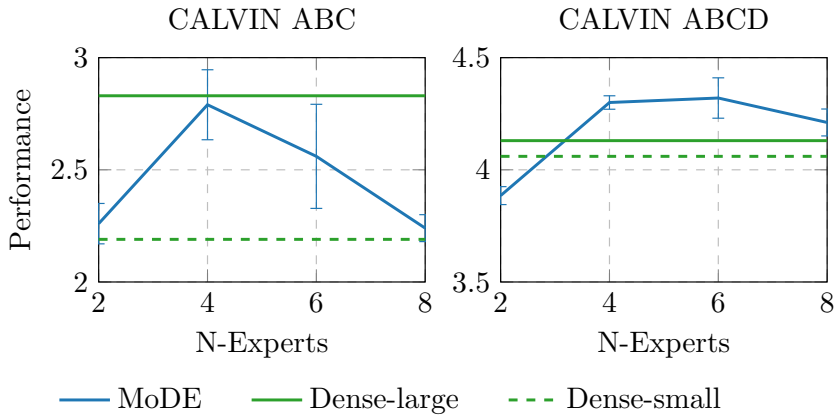

Figure 8: Scaling performance of MoDE and Dense-MoDE on CALVIN ABC and ABCD environments, showing average performance for 2 to 8 experts using best-performing variants for each environment.

2023). BESO uses the same continuous-time diffusion policy combined with a dense transformer to predict a single action given a sequence of prior states. To enable a fair comparison, we chose the same hyperparameters for BESO and MoDE in both settings. We test all models averaged over 4 seeds and report the mean values directly from prior work (Lee et al., 2024a).

Results. The results of both experiments are summarized in Table 8. MoDE achieves a new SOTA performance on both benchmarks and outperforms the dense transformer variant of BESO in both settings. Further, MoDE achieves higher performance compared to other policy representation methods such as VQ-BeT and C-BeT.

A.5.1 Mixture-of-Experts Ablations

Q: How does the Load Balancing Loss influence the Expert Distribution?

We analyze how the load balancing loss affects expert distribution across noise levels by training MoDE on LIBERO-10 with varying load balancing weights $\gamma_{LB} \in [0.1, 0.01, 0.001, 0.0001]$ Figure 9 visualizes the resulting expert distributions.

With a high load balancing loss of 0.1, experts are used almost uniformly across all layers with minor variations in two out of eight layers (Figure 11a). However, this enforced uniformity comes at a cost - the average performance drops to 0.9. This result suggests that enforcing equal expert usage across noise levels may constrain the model's learning capacity.

At 0.01, we observe a more flexible distribution while maintaining good overall expert utilization (Figure 11b). Within individual layers, expert usage varies from 10% to 40% in various layers. This enables for specialization while preventing any expert from becoming dominant. This configuration achieves the best average performance and provides evidence that moderate specialization benefits the policy most.

As we reduce γ_{LB} further to a range of $[0.001, 0.0001]$, the expert distribution gets worse and the model there is an expert collapse is happening for lb of 0.0001 in several layers (Figure 10c and Figure 10d). These values show, that a the load balancing weight is crucial to guarantee a good usage of all experts for the model. The lower performance of these models (0.86 for $\gamma_{LB} = 0.001$ and 0.83 for $\gamma_{LB} = 0.0001$) suggests that balanced expert participation is important for optimal Diffusion Policy performance.

Q: What happens with increased number of Experts? Next, we study the load balancing distribution for models that use more experts. Our experiments with 6 and 8 expert variants on LIBERO-10 reveal challenges in scaling beyond 4 experts. As shown in Figure 10, configurations with more experts consistently underutilize their capacity, with most layers actively using only 4 experts even with increased load balancing regularization (=0.1). These larger configurations also show decreased

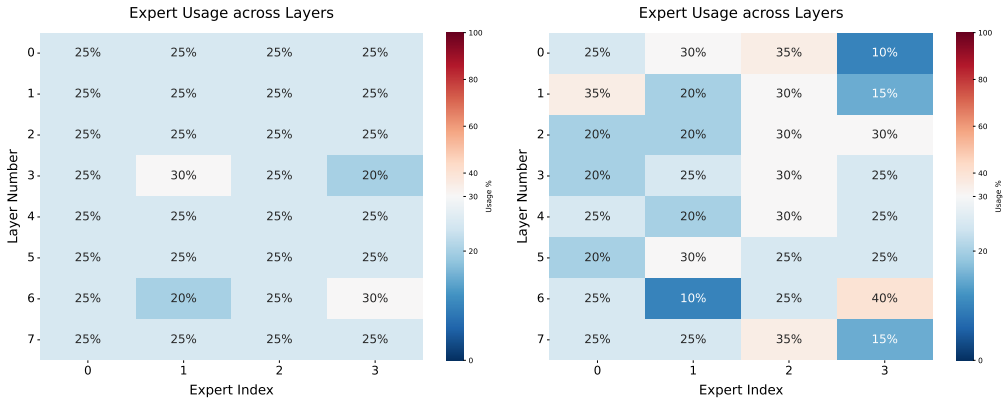

(a) $\gamma_{LB} = 0.1$ (b) $\gamma_{LB} = 0.01$

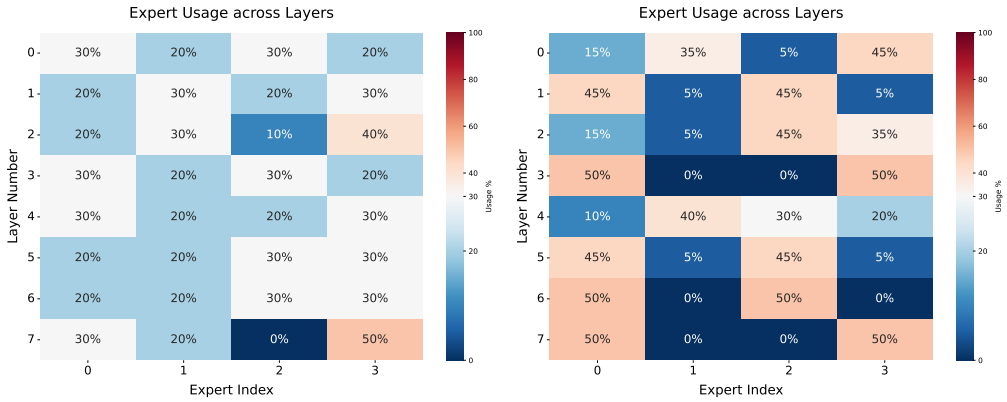

(c) $\gamma_{LB} = 0.001$ (d) $\gamma_{LB} = 0.0001$

Figure 9: Average Expert Utilization for different Load Balancing Weights across all denoising levels.

performance, indicating that 4 experts provides an optimal balance between representation capacity and learning efficiency. We hypothesize that additional experts impair the model's ability to learn effective representations from image and language inputs while maintaining noise-level specialization. This phenomenon persists even when increasing the load balancing loss factor, further supporting our finding that 4 experts offers the best trade-off between model capacity and performance.

Q: How is the expert distribution with topk=1? We further study the impact of using $top_k = 1$ for MoDE. We analyze MoDE's behavior with topk=1 routing, both with and without a shared expert, using 4 experts total. As visualized in Figure 11, topk=1 configurations struggle to maintain balanced expert utilization, typically collapsing to using only two of the four available experts. While this configuration shows only modest performance degradation on LIBERO-10, its impact is more visible on the challenging CALVIN ABC benchmark, where the average rollout length drops from 3.34 (topk=2) to 2.72 (topk=1). These results highlight the importance of expert interpolation across noise levels, with topk=2 providing the necessary flexibility to blend expert specializations for optimal performance.

Q: What expert distribution patterns emerge for different noise levels?

Finally, we analyze the different experts loads for various noise levels of our biggest model after pretraining on diverse robotics data. Detailed results are shown in Figure 12.

Our analysis of the expert distribution reveals several key insights about how the model learns to organize its mixture-of-experts architecture:

Noise-Level Specialization

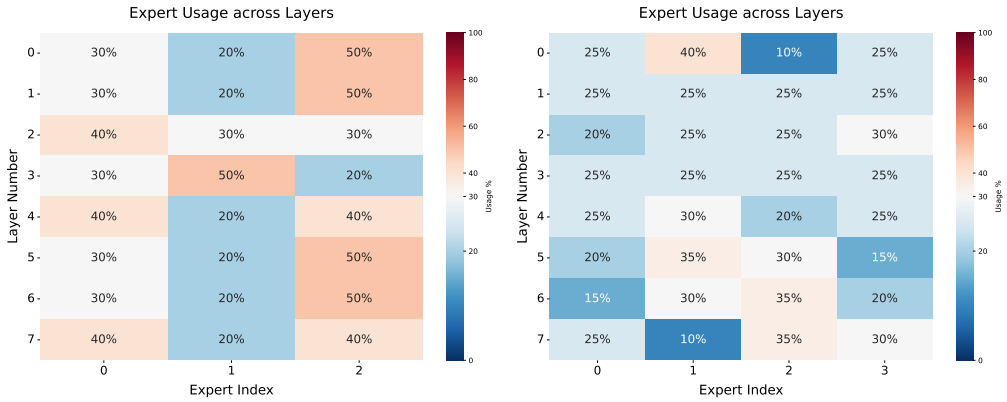

(a) 3 Experts

(b) 4 Experts

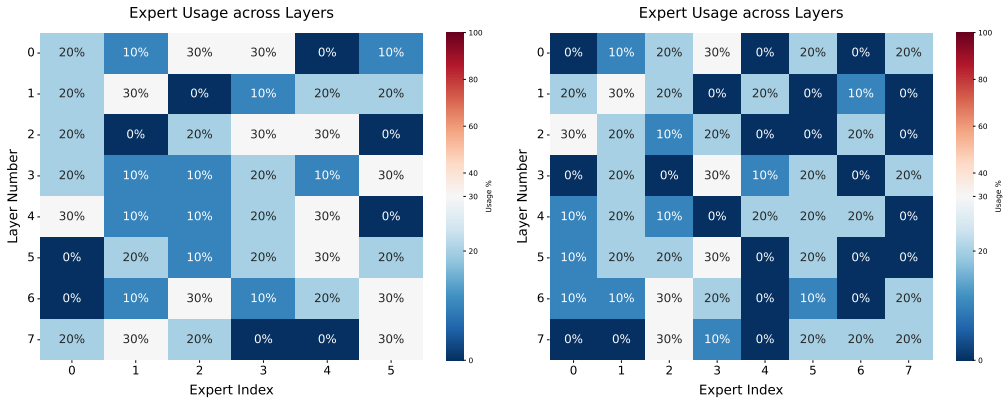

(c) 6 Experts

(d) 8 Experts

Figure 10: Average Expert Utilization for different number of used experts across all denoising levels.

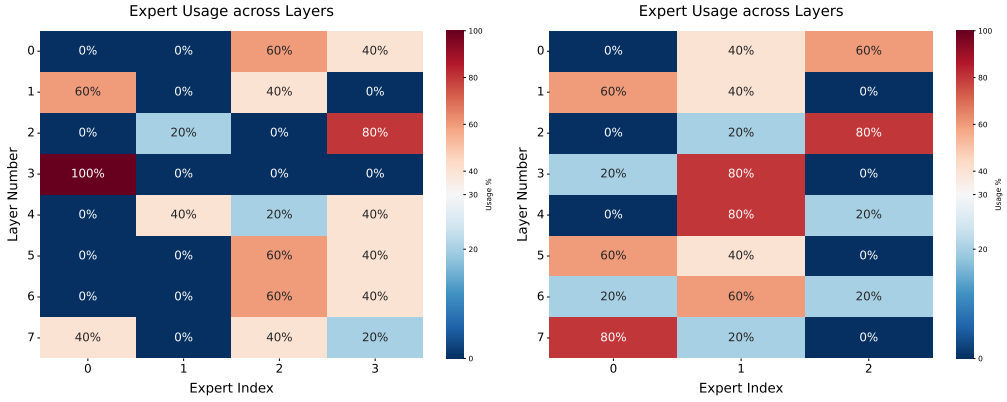

(a) topk=1

(b) topk=1 with shared Expert

Figure 11: Average Expert Utilization for two variants that use topk=1: left MoDE with 4 experts, right MoDE with 4 experts, where 1 is used in all settings as a shared one. Overall, MoDE struggles to equally distribute tokens across experts in this setting.

- – Experts specialize between high-noise (σ_1-σ_7) and low-noise (σ_8-σ_{10}) regimes, particularly visible in L4 where E3 and E0 show distinct high activation patterns in different noise regimes

  - Clear transition point around σ_8 where expert utilization patterns shift, most evident in L4 and L5 with stark changes in expert activation
  - Smooth handoff between denoising phases, exemplified in L7 where expert activations gradually transition across noise levels

- **Layer-wise Organization**
  - Early layers (L0-L4) show distinct expert specialization, particularly visible in L4's strong alternating expert patterns
  - Middle layers (L5-L7) demonstrate more distributed expert utilization, shown by more balanced activation patterns
  - Later layers (L8-L11) return to clearer specialization, evident in L11's distinct expert preferences
  - First layer (L0) shows particularly strong specialization for low-noise scenarios, with clear expert preferences in the final denoising steps

- **Expert Role Distribution**
  - Different experts develop specialized roles, most clearly visible in L4 where experts show strong preferences for specific noise ranges
  - Some experts consistently handle high-noise denoising (evident in L3 and L4) while others focus on low-noise refinement (for example in in L7-L8)
  - "Transitional experts" emerge in middle noise ranges, particularly visible in L5's balanced activation patterns
  - Model employs different expert combinations across layers, well demonstrated in the contrasting patterns between L4 and L8

- **Load Balancing Properties**
  - Effective load balancing achieved across experts, particularly visible in the distributed patterns of L5-L7
  - No single expert dominates across all noise levels, as shown by the varied activation patterns in each layer
  - Smooth transitions between noise regimes, most evident in the gradual activation changes in L4 and L5

These findings provide strong evidence that MoDE effectively partitions the denoising process across its experts, with each expert naturally specializing in different phases. The emergence of this organization without explicit supervision supports the effectiveness of our architectural choices and routing strategy.

A.6 Extended Related Work

MoE in Robotics. In the context of robotics, MoE models are used in many settings without being combined with a transformer architecture. Several works use a mixture of small MLP policies, that focus on different skills in Reinforcement Learning (Obando-Ceron et al., 2024; Celik et al., 2022; 2024) or for robot motion generation(Hansel et al., 2023; Le et al., 2023), another body of work utilizes combinations of small CNNs robot perception (Riquelme et al., 2021; Mees et al., 2016). Further applications include learning multimodal behavior using a mixture of Gaussian policies (Blessing et al., 2023; Li et al., 2023a). Despite the extensive usage of MoE in many domains, no prior work has tried to utilize MoE together with Diffusion Policies for scalable and more efficient Diffusion Policies.

Transformers for Robot Learning. Transformer models have become the standard network architecture for many end-to-end robot learning policies in the last few years. They have been combined with different policy representations in the context of IL. One area of research focuses on generating sequences of actions with Variational Autoencoder (VAE) models (Bharadhwaj et al., 2023; Zhao et al., 2023). These action-chunking transformer models typically use an encoder-decoder transformer

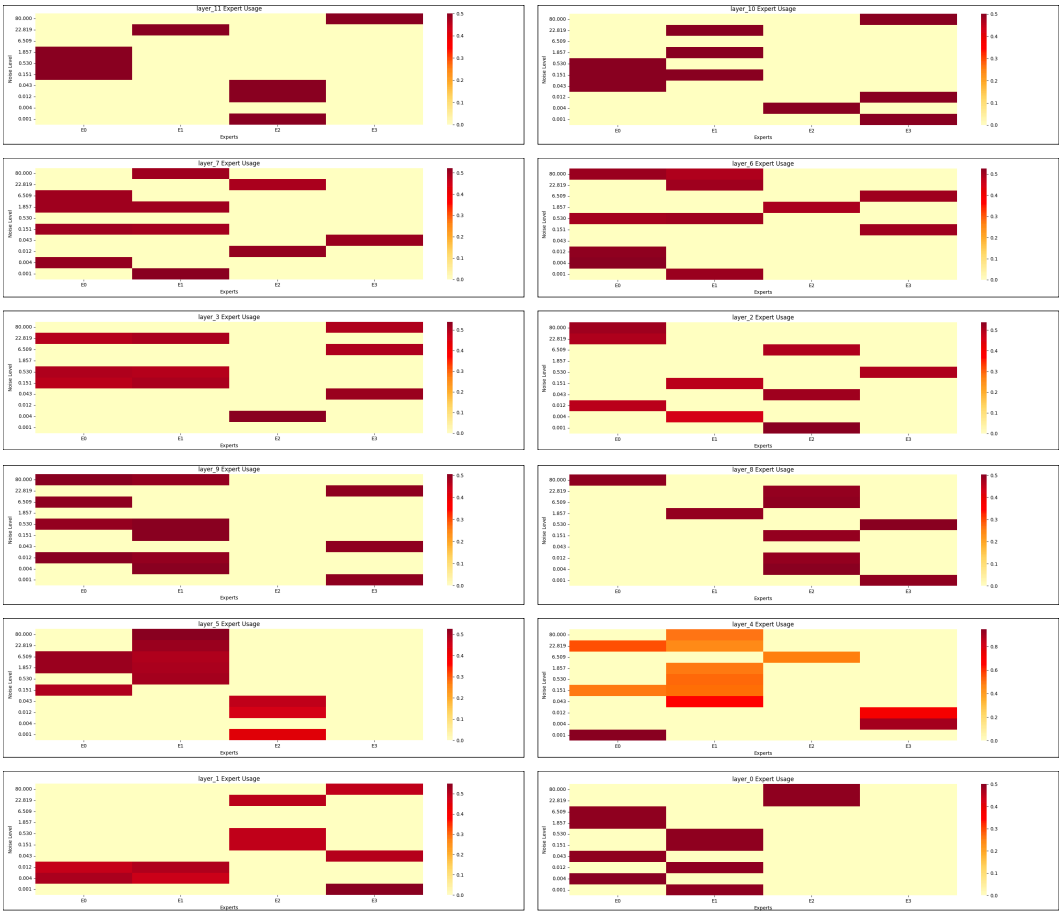

Figure 12: This image shows the expert usage distribution across 12 layers in a Mixture of Experts (MoE) model. Each subplot represents a different layer (from layer 0 to layer 11), with experts labeled E0, E1, E2, and E3 on the x-axis. The y-axis indicates the log-scaled token count, displaying the frequency of tokens routed to each expert within that layer. The color gradient indicates the proportion of tokens assigned to each expert, where darker colors represent higher usage.

as a policy architecture. Several Diffusion Policies, such as Octo (Octo Model Team et al., 2023), BESO (Reuss et al., 2023), ChainedDiffuser (Xian et al., 2023) and 3D-Diffusion-Actor leverage a transformer model as a policy backbone. Another direction of research treats behavior generation as discrete next-token predictions similar to auto-regressive language generation (Touvron et al., 2023). C-Bet, RT-1, and RT-2 use discretized action binning to divide seen actions into k-classes (Cui et al., 2023; Shafiullah et al., 2022; Brohan et al., 2022; Zitkovich et al., 2023), while VQ-BeT (Lee et al., 2024a) learns latent actions with residual Vector Quantization. Several works have shown the advantages of using pre-trained LLM or VLM as a policy backbone, which are then finetuned for action generation (Brohan et al., 2023; Gu et al., 2024; Collaboration et al., 2023; Li et al., 2024a). None of the recent work considers using any Mixture-of-Expert architecture for policy learning. MoDE is the first architecture to leverage MoE architecture combined with diffusion for behavior generation.